Interactions between main-channels and tributary alluvial fans: channel adjustments and sediment-signal propagation

Sara Savi[1], Stefanie Tofelde[1,2], Andrew D. Wickert[3], Aaron Bufe[2], Taylor F. Schildgen[1,2], and Manfred R. Strecker[1]

[1]Institut für Geowissenschaften, Universität Potsdam, 14476 Potsdam, Germany
[2]Helmholtz Zentrum Potsdam, GeoForschungsZentrum (GFZ) Potsdam, 14473 Potsdam, Germany
[3]Department of Earth Sciences and Saint Anthony Falls Laboratory, University of Minnesota, Minneapolis, MN 55455, USA

Corresponding Author: Sara Savi (savi@geo.uni-potsdam.de)

Abstract

Climate and tectonics impact water and sediment fluxes to fluvial systems. These boundary conditions set river form and can be recorded by fluvial deposits. Reconstructions of boundary conditions from these deposits, however, is complicated by complex channel-network interactions and associated sediment storage and release through the fluvial system. To address this challenge, we used a physical experiment to study the interplay between a main channel and a tributary under different forcing conditions. In particular, we investigated the impact of a single tributary junction, where sediment supply from the tributary can produce an alluvial fan, on channel geometries and associated sediment-transfer dynamics. We found that the presence of an alluvial fan may either promote or prevent sediment to be moved within the fluvial system, creating different coupling conditions. By analysing different environmental scenarios, our results reveal the contribution of both the main channel and the tributary to fluvial deposits

upstream and downstream of the tributary junction. We summarize all findings in a new conceptual framework that illustrates the possible interactions between tributary alluvial fans and a main channel under different environmental conditions. This framework provides a better understanding of the composition and architecture of fluvial sedimentary deposits found at confluence zones, which can facilitate the reconstruction of the climatic or tectonic history of a basin.

1. Introduction

The geometry of channels and the downstream transport of sediment and water in rivers are determined by climatic and tectonic boundary conditions (Allen, 2008, and references therein). Fluvial deposits and landforms such as conglomeratic fill terraces or alluvial fans may record phases of aggradation and erosion that are linked to changes in sediment or water discharge, and thus provide important archives of past environmental conditions (Armitage et al., 2011; Castelltort and Van Den Driessche, 2003; Densmore et al., 2007; Mather et al., 2017; Rohais et al., 2012; Tofelde et al., 2017). Tributaries are an important component of fluvial networks, but their contribution to the sediment supply of a river channel can vary substantially (Bull, 1964; Hooke, 1967; Lane 1955; Leopold and Maddock, 1953; Mackin, 1948; Miller, 1958). Their impact on the receiving river (referred to as *main channel* hereafter) may not be captured by numerical models of alluvial channels, as most models either parameterize the impacts of tributaries into simple relationships between drainage-basin area and river discharge (Whipple and Tucker, 2002; Wickert and Schildgen, 2019), or treat the main channel as a single channel with no lateral input (e.g., Simpson and Castelltort, 2012). Extensive studies on river confluences (e.g., Rice et al., 2008 and references therein) mainly focus on (1) hydraulic parameters of the water flow dynamics at the junction (Best 1986, 1988), which are relevant for management of infrastructure (e.g., bridges), and (2) morphological changes of the main channel bed, which are relevant for sedimentological studies and riverine habitats (Benda et al., 2004a; Best 1986; Best and Rhoads, 2008). Geomorphological changes (i.e., channel slope, width, or grain-size distribution) have been studied in steady-state conditions only (Ferguson et al., 2006; Ferguson and Hoey, 2008), and with no focus on fluvial deposits related to the interactions between

tributaries and the main channel. In source-to-sink studies an understanding of these processes, however, is relevant for the reconstruction of the climatic or tectonic history of a certain basin.

By modulating the sediment supplied to the main channel, tributaries may influence the distribution of sediment within the fluvial system, the duration of sediment transport from source areas to depositional basins (Simpson and Castelltort, 2012), and the origin and amount of sediment stored within fluvial deposits and at confluence zones. Additionally, complex feedbacks between tributaries and main channels (e.g., Schumm, 1973; Schumm and Parker, 1973) may enhance or reduce the effects of external forcing on the fluvial system, thus complicating attempts to reconstruct past environmental changes from these sedimentary deposits.

The dynamics of alluvial fans can introduce an additional level of complication to the relationship between tributaries and main channels. Fans retain sediment from the tributary and influence the response of the connected fluvial system to environmental perturbations (Ferguson and Hoey, 2008; Mather et al., 2017). Despite the widespread use of alluvial fans to decipher past environmental conditions (Bull, 1964; Colombo et al., 2000; D'Arcy et al., 2017; Densmore et al., 2007; Gao et al., 2018; Harvey, 1996; Savi et al., 2014; Schildgen et al., 2016), we lack a clear understanding of the interactions between alluvial fans and main channels under the influence of different environmental forcing mechanisms. This knowledge gap limits our understanding of (1) how channels respond to changes in water and sediment supply at confluence zones, and (2) how sediment moves within fluvial systems (Mather et al., 2017; Simpson and Castelltort, 2012), with potential consequences for sediment-transport dynamics as well as for the composition and architecture of fluvial sedimentary deposits.

In this study, we analyze the interplay between a main channel and a tributary under different environmental forcing conditions in an experimental setting, with particular attention to tributaries that generate an alluvial fan. Physical experiments have the advantage of providing a simplified setting with controlled boundary conditions that may include water and sediment discharge, and uplift rate or base-level changes. These models may thus capture many components of complex natural behaviors (Hooke, 1967; Paola et al., 2009; Schumm and Parker, 1973), and they provide an opportunity to analyze processes at higher spatial and temporal

resolution than is generally possible in nature (e.g., De Haas et al., 2016; Parker, 2010; Reitz et al., 2010) and to directly observe connections between external perturbations (e.g., tectonic or climatic variations) and surface processes impacting landscapes.

We present results from two groups of experiments in which we separately imposed a perturbation either in the tributary only (Group 1, Fig. 1a, b) or solely in the main channel (Group 2, Fig. 1c). Group 1 can be further subdivided into cases in which the tributary has: (a) an aggrading alluvial fan (Fig. 1a) or (b) an incising alluvial fan (Fig. 1b). In this context, we distinguish between two modes of fan construction: *fan aggradation*, i.e., deposition of material on the fan surface, which leads to an increase in the fan surface elevation, and *fan progradation*, i.e., deposition that occurs at the downstream margin of the fan, which leads to fan lengthening. Progradation may occur during both aggradation and incision phases (Fig. 1). Group 2, in contrast, represents the case of a sudden increase in water discharge in the main channel (Fig. 1c), as for example related to an increase in glacial melt.

By analyzing how a tributary may affect the main channel under these different forcing conditions, we aim to build a conceptual framework that lends insight into the interplay between alluvial fans and main channels. Toward this goal, we provide a schematic representation of how the downstream delivery of sediment changes under different environmental conditions. Through this representation, we hope to contribute to a better understanding and interpretation of fluvial morphologies and sedimentary records, which may hold important information about regional climatic and tectonic history (Allen, 2008; Armitage et al., 2011; Castelltort and Van Den Driessche, 2003; Densmore et al., 2007; Mather et al., 2017; Rohais et al., 2012).

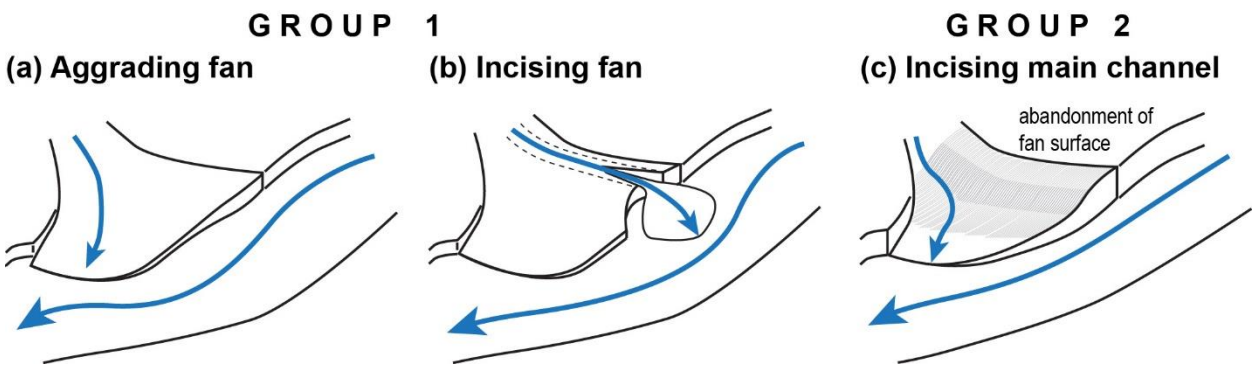

Figure 1. Schematic representation of the three scenarios analyzed in this study.

2. Background

2.1. Geometry and sediment transfer dynamics in a single-channel system

An alluvial river is considered to be in steady state when its water discharge provides sufficient power, or sediment-transport capacity, to transport the sediment load supplied from the upstream contributing area at a given channel slope (Bull, 1979; Gilbert, 1877; Lane, 1955; Mackin, 1948). When a perturbation occurs in the system, the river must transiently adjust one or more of its geometric features (e.g., slope, width, depth, or grain-size distribution) to re-establish equilibrium (Mackin 1948; Meyer-Peter and Müller, 1948). Slope adjustments are not uniform along the channel. If the perturbation occurs in the basin's headwater (e.g., a change in water or sediment supply), slope adjustments propagate downstream from the channel head (Simpson and Castelltort 2012; Tofelde et al., 2019; Van den Berg Van Saparoea and Potsma, 2008; Wickert and Schildgen, 2019). In contrast, slope adjustments propagate upstream if a perturbation occurs toward the downstream end of the channel (e.g., a change in base level) (Parker et al., 1998; Tofelde et al., 2019; Van den Berg Van Saparoea and Potsma, 2008; Whipple et al., 1998). The sediment transport rate of the river also depends on the direction of the change, as an increase or a decrease in precipitation or uplift rates trigger opposite responses (i.e., increase or decrease in sediment transport rate; Bonnet and Crave, 2003).

2.2. Geometry and sediment-transfer dynamics in a multi-channel system

2.2.1. Tributary influence on main channel

At confluence zones, the main channel is expected to adapt its width, slope, sediment transport rate, and sediment-size distribution according to the combined water and sediment supply from the main channel and the tributary (Benda et al., 2004b; Best, 1986; Ferguson et al., 2006; Lane 1955; Miller, 1958; Rice et al., 2008). Consequently, a perturbation occurring in the tributary will also affect the main channel. In their numerical model, Ferguson et al. (2006) explored the effects that changes in sediment supplied from a tributary have on the main

channel's slope. They found that when tributaries cause aggradation at the junction with the main channel, the main channel slope adjustments extend approximately twice as far upstream as they do downstream. They additionally found that variations in grain size of the tributary influence the grain-size distribution in the main channel, both upstream and downstream of the tributary junction. Because we used a homogeneous grain size in our experiments, the work of Ferguson et al. (2006) complements our analyses.

Whether the tributary is aggrading, incising, or in equilibrium may also have important consequences for *how* and *where* local fluvial deposits (i.e., alluvial-fan deposits or fluvial terraces) reflect environmental signals. For example, when sediment is trapped within a tributary's alluvial fan, the fan acts as a *buffer* for the main channel, and environmental signals do not propagate from the tributary into the fluvial deposits of the main channel (Ferguson and Hoey, 2008; Mather et al., 2017). In contrast, where the tributary and main channel are fully *coupled* (i.e. all sediment mobilized in the tributary reaches the main channel), the signal transmitted from the tributary can be recorded in the stratigraphy of the main river (Mather et al., 2017). The presence of an alluvial fan may additionally cause a change in the main river location, pushing it against the opposite side of the valley. This allows the fan to grow more in the downstream direction of the main flow, contributing to a strong asymmetry in its morphology that may be preserved in the stratigraphic record of the flood plain (Giles et al., 2016).

2.2.2. Main channel influence on tributary

The main channel influences a tributary primarily by setting its local base level. Therefore, a change in the main-channel bed elevation through aggradation or incision represents a downstream perturbation for the tributary, and tributary-channel adjustments will follow a *bottom-up* propagation direction (Mather et al., 2017; Schumm and Parker, 1973). Typically, a lowering of the main channel produces an initial phase of tributary-channel incision (Cohen and Brierly, 2000; Fulkner et al., 2016; Germanoski and Ritter, 1988; Heine and Lant, 2009; Ritter et al., 1995; Simon and Rinaldi, 2000), followed by channel widening (Cohen and Brierly, 2000; Germanoski and Ritter, 1988), which occurs through bank erosion and mass-wasting processes (Simon and Rinaldi, 2000). As base-level lowering continues, the fan may become entrenched, with the consequent abandonment of the fan surface and renewed deposition at a lower elevation

(Clark et al., 2010; Mather et al., 2017; Mouchené et al., 2017; Nicholas et al., 2009) (Fig. 1c). In contrast, aggradation of the main channel may lead to tributary-channel backfilling and avulsion (Bryant et al., 1995; De Haas et al., 2016; Hamilton et al. 2013; Kim and Jerolmack, 2008; Van Djik et al., 2009, 2012).

When a non-incising main channel (*non-incising main axial river* of Leeder and Mack, 2001) is characterized by efficient lateral erosion, it can efficiently erode the fan downstream margin, thereby "cutting" its toe (Larson et al., 2015) (*fan-toe cutting* hereafter) (Fig. 1b). This toe-cutting generally occurs in the up-valley side of the fan and thus shortens it (Giles et al., 2016).) As a consequence, the tributary channel-slope increases and so does its transport capacity, which triggers an upstream-migrating wave of incision. Fan-toe cutting may thus cause fan incision and a consequent increase in sediment supply from the tributary to the main channel (*healing wedge* hereafter; Leeder and Mack, 2001), in a process similar to that caused by an incising main channel (*incising main axial river of* Leeder and Mack, 2001).

3. Methods

3.1. Experimental setup

We conducted physical experiments at the Saint Anthony Falls Laboratory (Minneapolis, USA). The experimental setup consisted of a wooden box with dimensions of 4 m x 2.5 m x 0.4 m, which was filled with quartz sand with a mean grain size of 144 μm (standard deviation of 40 μm). Two separate water and sediment input zones were used to form a main channel (MC) and a tributary channel (T) (Fig. 2a). The main channel's input zone was located along the short side of the box, whereas the tributary's input zone was located along the long side at a distance of 1.7 m downstream of the main-channel inlet (Fig. 2a). This setting represents a landscape with two transport-limited streams that join in a broad alluvial valley of unlithified/uncemented sediments; common for many arid regions with large flood plains. A simplification in our experiments is that the grain sizes from both the main stem and the tributary are equal. This will be further discussed in section 5.4. For each of the two input zones, the water supply (Q_w) and sediment supply (Q_{s_in}) could be regulated separately, and sand and water were mixed before entering the box by feeding them through cylindrical wire-mesh diffusers filled with gravel. Before entering

the mesh, water was dyed blue to be visible on photos. At the downstream end, sand (Q_{s_out}) and water exited the basin through a fix 20 cm-wide gap that opened onto the floor below. This downstream sink was required to avoid deltaic sediment deposition that would, if allowed to grow, eventually raise the base level of the fluvial system. At the beginning of each experiment, an initial channel was shaped by hand to allow the water to flow towards the outlet of the box.

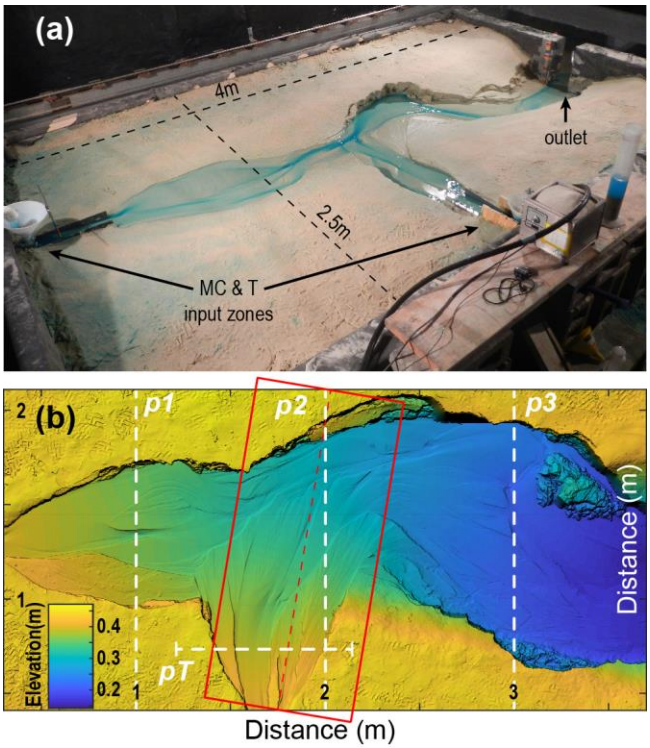

Figure 2. Experimental set-up. (a) Wooden box for the experiments showing the two zones of sediment and water input, and the outlet of the basin. (b) Digital elevation model constructed from laser scans (1 mm horizontal resolution). Red box shows the area of the swath grid used for the calculation of the tributary long profile (Fig. 4) and slope values. Dashed white lines represent the location of the cross sections shown in Figs. 5 and S1 of the Supplementary Material.

3.2. Boundary conditions

We performed six experiments with different settings and boundary conditions to simulate different tributary–main-channel interactions (Table 1). As a reference, we included one experiment without a tributary and with a constant Q_{s_in} and Q_w (MC_NC, where MC stands for

Main Channel only and the suffix NC stands for *No Change* in boundary conditions; reported in Tofelde et al., 2019 as the Ctrl_2 experiment). The other five experiments all have a tributary and are divided into two groups: In Group 1, Q_w and Q_{s_in} on the main channel were held constant, whereas we varied these inputs to the tributary. In Group 2, Q_w and Q_{s_in} on the tributary were held constant, whereas we increased Q_w in the main channel. In natural systems, changes in water and sediment supply may affect the main channel and tributary simultaneously, but to isolate the effects of the main channel and the tributary on each other, we studied perturbations that only affect one of them at a time. Our results can be combined to predict the response to a system-wide change in boundary conditions.

Each group includes one experiment with no change (NC) in Q_{s_in} and Q_w (T_NC1 and T_NC2, where T stands for *run with Tributary* and the numbers at the end correspond to the group number). Group 1 includes one experiment with an increase followed by a decrease in Q_{s_in} in the tributary (T_ISDS, where ISDS stands for *Increasing Sediment Decreasing Sediment*) and one experiment with a decrease followed by an increase in Q_w in the tributary (T_DWIW, where DWIW stands for *Decreasing Water Increasing Water*). Changes were first made in the direction that favored sediment deposition and the construction of an alluvial fan. Group 2 includes one experiment with no change (T_NC2) and one with an increase in Q_w in the main channel (T_IWMC, where IWMC stands for *Increasing Water in Main Channel*). Importantly, the initial settings of the two groups of experiments are different (Table 1). The Q_{s_in} and Q_w values were defined based on a set of preliminary test-runs and chosen to balance sediment transport and sediment deposition. In particular, initial Q_w and Q_{s_in} of Group 2 guarantee a higher Q_s/Q_w ratio compared to Group 1, so that we could evaluate the effects of a change in the main-channel regime (from a *non-incising main river* to an *incising main river*) on the tributary and on sediment-signal propagation. In the context of this coupled tributary–main-channel system, we explore: 1) the geometric variations that occur in the main channel and in the tributary (e.g., channel slope and valley geometry); and 2) the downstream delivery of sediment and sedimentary signals.

Table 1. Overview of input parameters.

	Initial conditions	**1st change**	**2nd change**	**Run time (spin-up)**

EXP NAME	MC		T		MC	T		T		
	Qw	Qs_in	Qw	Qs_in	Qw	Qw	Qs_in	Qw	Qs_in	
	mL/s	mL/s	mL/s	mL/s	mL/s	mL/s	mL/s	mL/s	mL/s	min
MC_NC**	95	1.3								690 (100)
Non-incising mean axial rivers – Group1					***(at 300 min)***			***(at 375* or 480 min)***		
T_NC1	95	1.3	63	2.2						600 (150)
T_ISDS	95	1.3	63	2.2			4.5		2.2	720 (150)
T_DWIW*	95	1.3	63	2.2		31.5		63		690 (150)
Incising mean axial rivers - Group2					***(at 180 min)***					
T_NC2	63	1.3	41.5	2.2						480 (100)
T_IWMC	63	1.3	41.5	2.2	126					480 (100)

* In the T_DWIW run the boundary condition change occurred at 375 min rather than 480 min as in the T_ISDS experiment because fast aggradation that occurred at the tributary input zone risked to overtop the wooden box margins.

**, Experiment published by Tofelde et al. (2019).

3.3. Measured and calculated parameters

3.2.1. Long profiles, valley cross-sections, and slope values

Every 30 min we stopped the experiments to perform a scan with a laser scanner mounted on the railing of the basin that surrounded the wooden box. Digital elevation models (DEMs) created from the scans have a resolution of 1 mm (Fig. 2b). We extracted long profiles and valley cross sections from these DEMs (i.e., elevation profiles perpendicular to the main flow direction) for the main channel and the tributary. Long profiles for the main channel were calculated by extracting the lowest elevation point along each cross section in the flow direction. Long profiles for the tributary were calculated with a similar procedure using outputs from Topotoolbox's SWATH profile algorithm (Schwanghart and Scherler, 2014) at 1 mm spatial resolution along the line of the average flow direction (Fig. 2b). By plotting elevation against down-valley or down-fan distance, rather than along the evolving path of the channels, the resulting slopes are slightly overestimated due to the low sinuosity of the channels. Cross sections were extracted at fixed positions, perpendicular to the main flow direction, for both the main channel and the tributary (Fig. 2b).

For the main channel, spatially-averaged slopes were additionally calculated by manually measuring the bed elevation at the inlet and at the outlet of the wooden box at 10-minute intervals during the experiments. This procedure yielded real-time estimates of channel slope. For comparison, spatially-averaged slopes where subsequently calculated also for the tributary channel using the maximum and minimum elevation of the tributary long profile calculated within the SWATH grid. Slope data are reported in the supplementary material.

3.2.2. Active valley-floor width and symmetry

We defined the width of the active valley floor as the area along the main channel that was occupied at least once by flowing water. It was measured along the main channel both upstream and downstream of the tributary junction (Fig. 3a, upper panel). The active valley floor was isolated by extracting all DEM values with an elevation of <0.42 m (where 0.42 m is the elevation of the sand surface outside the manually-shaped channel) and with a slope of <15 degrees (a value visually selected from the DEMs as the best cut-off value for distinguishing the valley floor from the banks). The average valley-floor width was then calculated as the average sum of pixels in each of the 700 cross sections within the selected zones (i.e., upstream or downstream of the tributary junction; Fig. 3a, upper panel). The same method was used to monitor valley axial symmetry. In this case, the averaged width was limited to the sum of pixels to the left and to the right of an imaginary central line crossing the basin from the inlet to the outlet (Fig. 3a). Small differences between left and right sums indicate high symmetry.

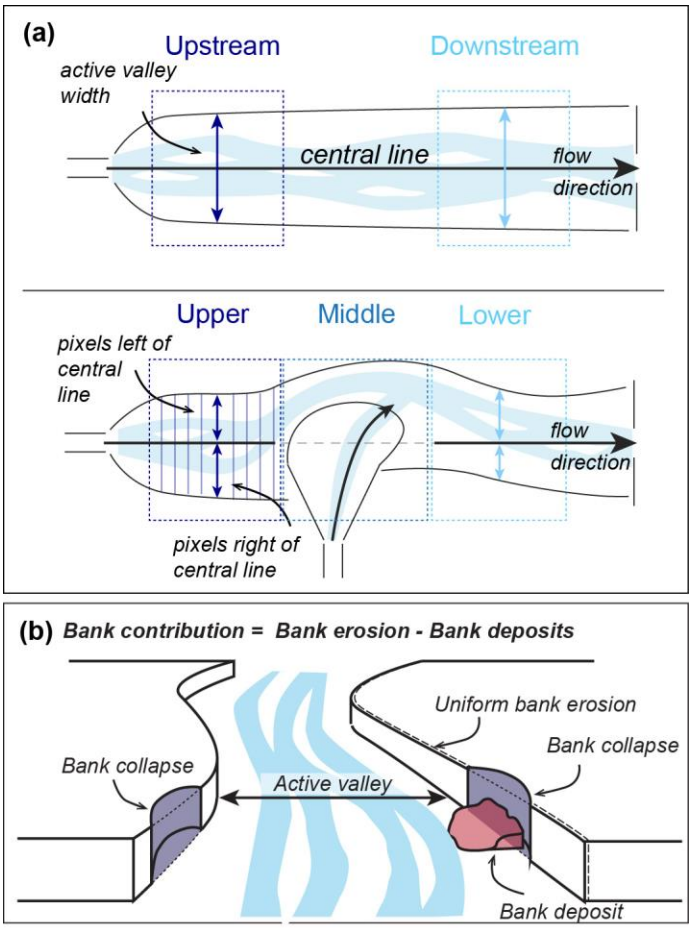

Figure 3. (a) Schematic representation of the method used to calculate the active valley width and axial symmetry. Symmetry and averaged width values are calculated for 700 cross sections located within the boxes marked in the upper panel. The averaged position of the valley margins with respect to an imaginary central line, which connects the source zone to the outlet of the wooden box, is shown in Figure 6. This representation highlights the symmetry of the valley and indirectly provides the valley width (i.e., sum of the right and left-margin positions). Boxes marked in the lower panel show the division into Upper, Middle, and Lower sections used for the calculation of the mobilized volumes (Fig. 8). (b) Schematic representation of the method used to calculate bank contribution: Elevation difference > -2.5 cm represents bank erosion and bank collapses, whereas differences > 2.5 cm represent large bank deposits. The contribution of the banks is calculated by subtracting these two values.

3.2.3. Sediment discharge at the outlet (Q_{s_out}), mobilized volumes, and bank contribution

The sediment discharge at the outlet of the basin (Q_{s_out}) was manually recorded at 10-minute intervals by measuring the volume of sediment that was collected in a container over a 10-second period. Q_{s_out} was also calculated by differencing subsequent DEMs (generating a "DEM of Difference", or DoD) and calculating the net change in sediment volume within the DEM. Although having a lower temporal resolution than the manual measurements (i.e., DoDs are averaged over 30 minutes), this DEM-based calculation allowed us to identify zones of aggradation and incision within the system and to calculate their volumes. For each DoD, we distinguished between changes along the active valley floor due to channel dynamics (elevation difference < 2.5 cm, value chosen as best cut-off value) and changes that occur along the channel and valley walls, for example due to bank collapses (elevation difference > 2.5 cm). Changes within the active valley floor were further divided into areas of net *aggradation* ($\Delta V_{vf} > 0$) and net *erosion* ($\Delta V_{vf} < 0$). Changes in bank elevation were divided into net *bank deposition* ($\Delta V_b > 0$) and net *bank collapses* or *erosion* ($\Delta V_b < 0$). These were used to calculate the bank contribution (V_b) to the total volume (V) of mobilized sediment (Fig. 3b). We separated the upper, middle, and lower sections of the experimental river valley by dividing the DEMs into three different zones (Fig. 3a, lower panel). For each section, we calculated the net change in sediment volumes between two time steps within the active valley floor (V_{vf}), along the banks (V_b), and the sum of the two contributions ($V = V_{vf} + V_b$).

The volumes are normalized to the Q_{s_in} measured over 30 minutes (to match the 30-minute period of a DoD). Negative V values indicate net incision, whereas positive values indicate net aggradation. V values close to zero may indicate that there was no change, or that the net incision ≅ net aggradation. As such, it is important to look at the variations through time rather than at single values.

4. Results

All experiments included an initial adjustment phase characterized by high Q_{s_out} and a short and rapid increase in the main-channel slope through preferential channel incision at the downstream end of the main channel. This phase represents the adjustment from the manually constructed valley shape to the shape that is equilibrated to the imposed boundary conditions. At the start of the adjustment phase, the channel rapidly incised toward the outlet, which was much lower than the height of the manually constructed valley bottom. Meanwhile, the channel deposited material at the channel head, adjusting to the Q_{s_in} and Q_w values. Analogous to a base-level fall observed in nature, these changes caused an increase in main-channel slope near the outlet and the upstream migration of a diffuse knick-zone that lowered the elevation of the main channel. After this initial adjustment, which marks the end of the spin-up phase, the main controlling factors for the shape of the channel were the Q_{s_in} and Q_w values only.

4.1. Geometric adjustments

Following the spin-up phase, channel-slope adjustments in our experiments matched the theoretical models described above (Section 2.1). The main-channel slope decreased in all experiments through incision at the upstream end, except for T_NC2 and the initial phase of T_IWMC, in which the boundary conditions favored aggradation (Fig. 4, Table 1). The slope of the tributary increased during periods of fan aggradation (e.g., IS phase of the T_ISDS run, and DW phase of the T_DWIW run) and decreased during periods of fan incision (DS phase of the T_ISDS run, and IW phase of the T_DWIW run) (Fig. 4). Slope adjustments did not occur uniformly, but followed a top-down or bottom-up direction depending on the origin of the perturbation (e.g., changes in headwater conditions or base-level fall at the tributary outlet).

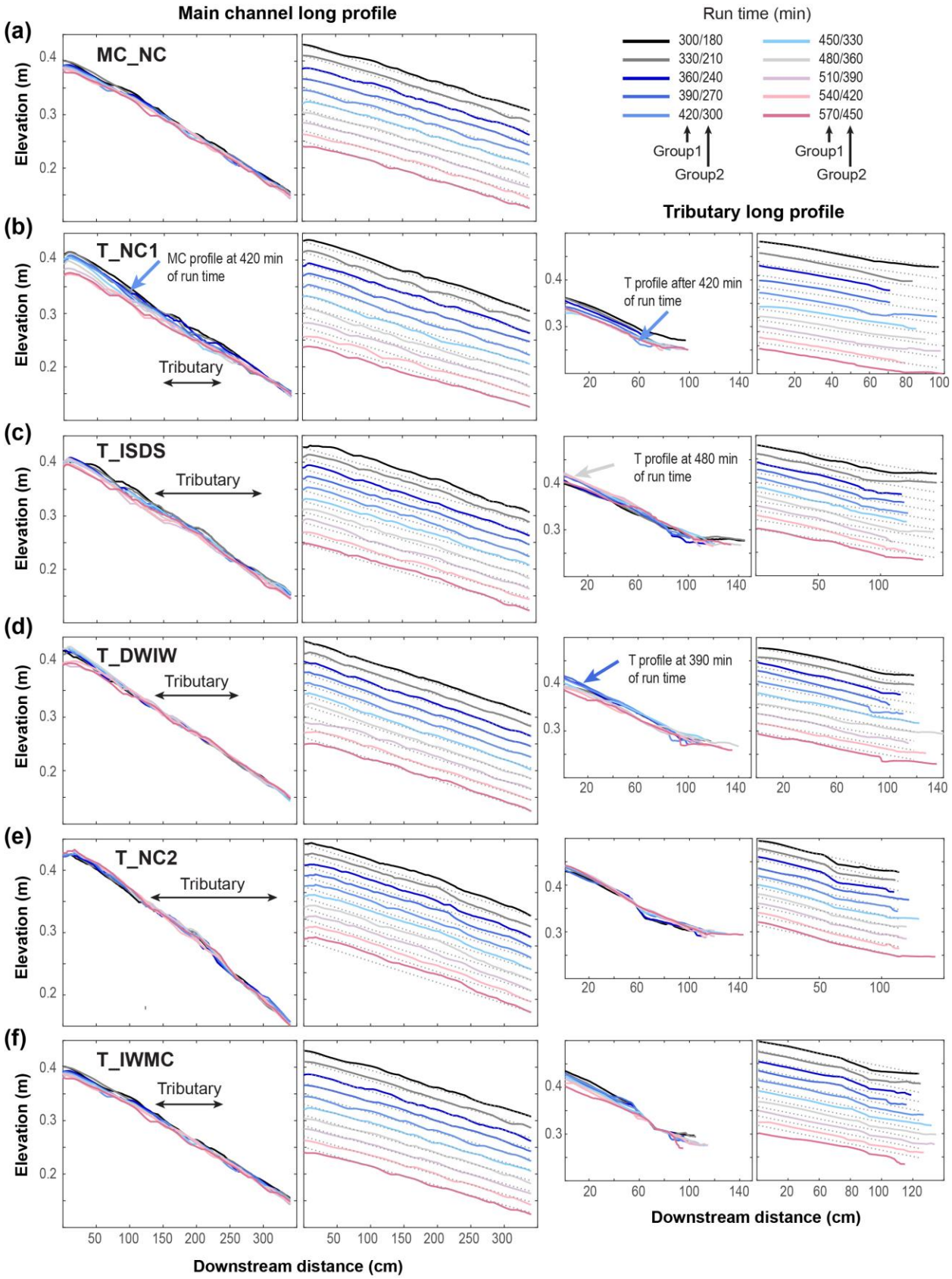
Main channel long profile
Run time (min)
300/180
330/210
360/240
390/270
420/300
450/330
480/360
510/390
540/420
570/450
Group1
Group2
Group1
Group2
Tributary long profile
(a)
MC_NC
(b)
T_NC1
MC profile at 420 min of run time
Tributary
T profile after 420 min of run time
(c)
T_ISDS
Tributary
T profile at 480 min of run time
(d)
T_DWIW
Tributary
T profile at 390 min of run time
(e)
T_NC2
Tributary
(f)
T_IWMC
Tributary
Elevation (m)
Downstream distance (cm)
Downstream distance (cm)

336

Figure 4. Long profiles of the main channel (left panels) and of the tributary channel (right panels) for all runs. Profiles represent the experiments between 300 and 570 minutes for the MC_Ctrl2, T_NC1, T_ISDS, and T_DWIW runs (legend values to the left of the slashes), and between 180 and 450 minutes for the T_NC2, and T_IWMC runs (legend values to the right of the slashes). For both the main and the tributary channel, left panels show the topographic evolution of the channels with time, whereas right panels show a single profile (i.e., at a specific time) compared to the average slope of the first plotted profile. Along the main channel profiles, horizontal arrows indicate the position and extent of the tributary channel/alluvial fan, whereas colored arrows indicate the position of the channels in particular run times discussed in the text.

Valley width in both the main channel (Fig. 5) and the tributary (Fig. S1 of the Supplementary Material) increased during the experiments through bank erosion and bank collapses, until reaching relatively steady values (Fig. 6). The experiments with the tributary (Fig. 6b – f) developed a much wider main-channel valley, especially downstream of the tributary, due to higher total Q_w compared to the main channel only experiments. In these experiments, valleys were also strongly asymmetrical, with more erosion affecting the valley side opposite the tributary (Figs. 5 and 6).

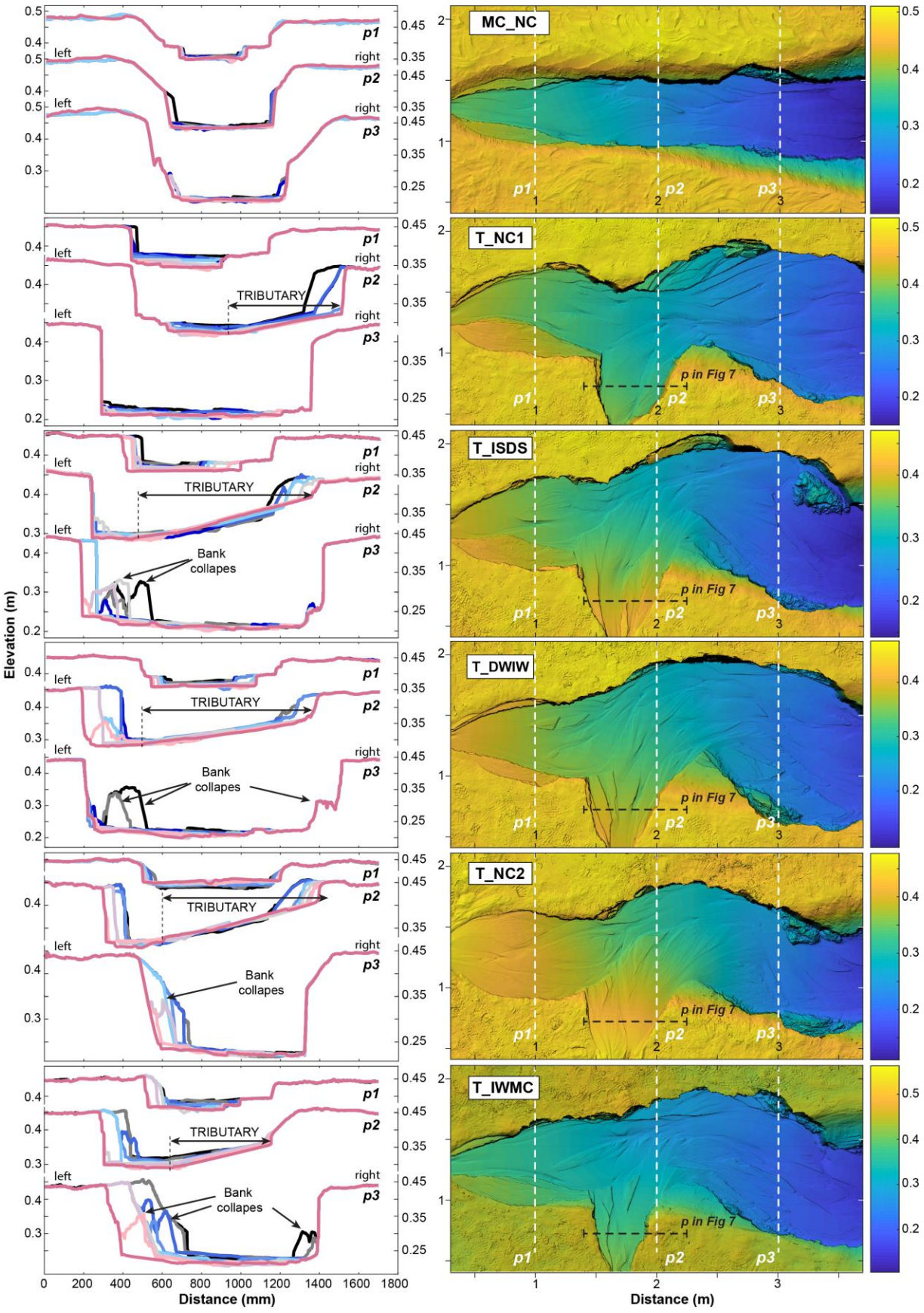
MC_NC
T_NC1
T_ISDS
T_DWIW
T_NC2
T_IWMC
p1
p2
p3
left
right
TRIBUTARY
Bank collapes
p in Fig 7
Elevation (m)
Distance (mm)
Distance (m)

355

Figure 5. Left panels: Cross sections obtained from the DEMs at three different locations along the main channel (p1, p2, and p3 respectively). The color code represents successive DEMs as illustrated in Fig. 4 (i.e., same colors for the same run times). All cross sections are drawn from left to right looking in the downstream direction. Right panels: DEM maps expressed in meters; color code represents the elevation with respect to the channel floor (also in meters).

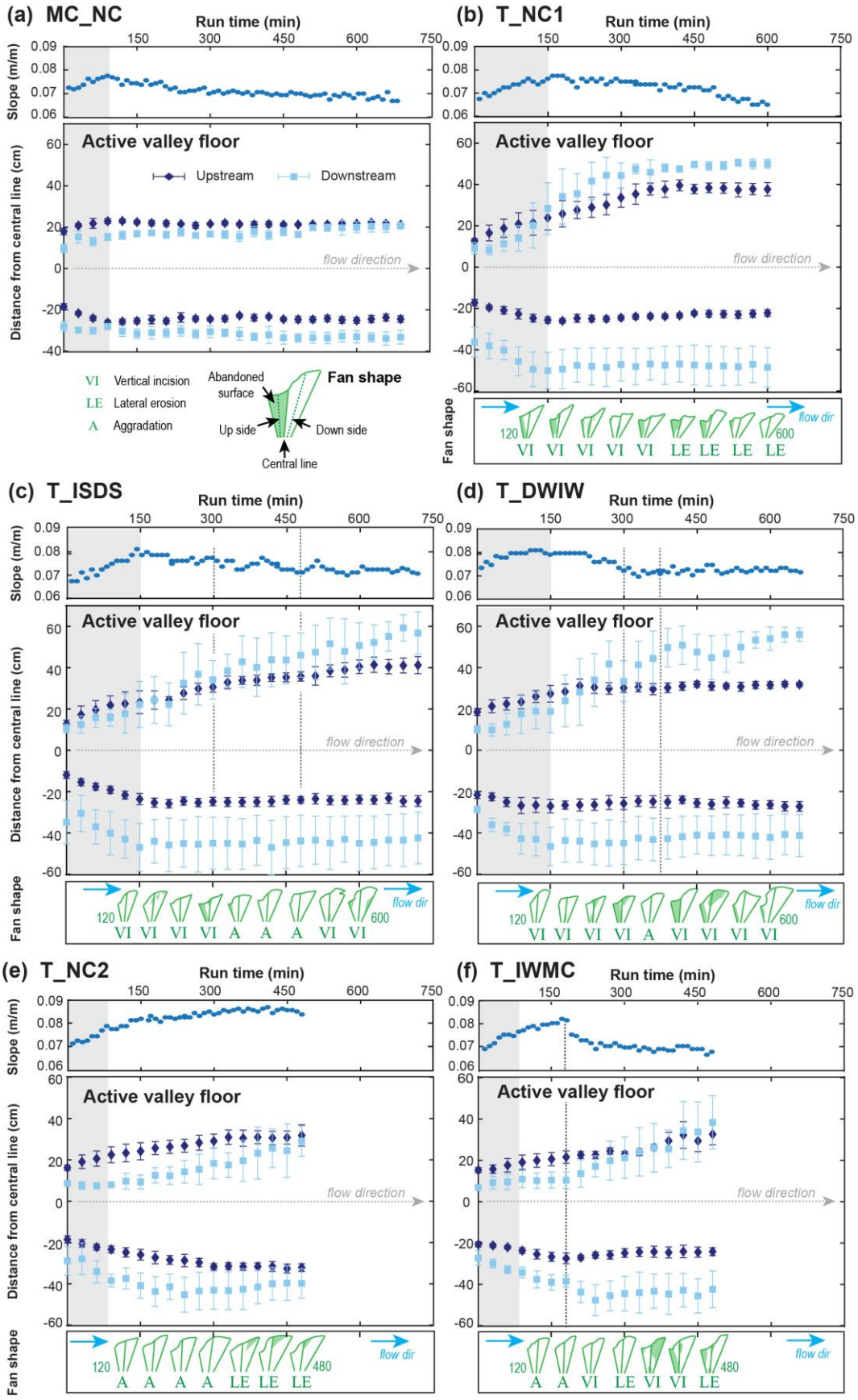
(a) MC_NC
(b) T_NC1
(c) T_ISDS
(d) T_DWIW
(e) T_NC2
(f) T_IWMC
Run time (min)
Slope (m/m)
Active valley floor
Distance from central line (cm)
Upstream
Downstream
flow direction
VI Vertical incision
LE Lateral erosion
A Aggradation
Abandoned surface
Fan shape
Up side
Down side
Central line
Fan shape
flow dir

Figure 6. Variations in the geometry of the active valley floor for all experiments. For each experiment the upper panel shows the measured slope (measured every 10 minutes during each experimental run). The middle panel shows the calculated average position of the right and left valley margins with respect to the central line, respectively for the main channel upstream and downstream of the tributary junction (as indicated in Fig. 3a). Gray areas represent the spin-up phase of each experiment (based on the break-in-slope registered through the manual slope measurements; (a–f) upper panels). Vertical dotted lines in the T_ISDS, T_DWIW, and T_IWMC runs represent the *time of change* in boundary conditions. Values are reported with their relative 1σ value. For all experiments with a tributary, the shape of the fan and the dominant sedimentary regime acting in the tributary at that specific time (i.e., vertical incision (VI), lateral erosion (LE), or aggradation (A)) are shown in the lower panel. In all experiments, fan-toe cutting (Leeder and Mack, 2001; Larson et al., 2015) mainly occurred at the upstream margin of the fan and contributed to the strong asymmetry of the fan morphology (Table S9 of Supp. Material), similar to what has been observed in nature (Giles et al., 2016).

4.2. Q_{s_out} and bank contribution

Our experiments offered an opportunity to evaluate the impacts of sediment supply from the tributary to the main channel through space and time. In general, sediment moved in pulses, and areas of deposition and incision commonly coexisted (Fig. 7a).

Q_{s_out} varied greatly, but generally decreased through time (the only exception is the T_IWMC run, where Q_{s_out} remained high) (Fig. 7, black circles). Values for the mobilized sediment, V, calculated from the DoDs (averaged over 30 minutes) show similar trends, but with a lower variability that reflects the long-term average Q_{s_out} (Fig. 7, black lines). An appreciable reduction of Q_{s_out} occurred when the system was approaching equilibrium (e.g., end of Fig. 7a, b) and during times of fan aggradation in the tributary (i.e., IS and DW phases of Fig. 7c, d, and e). Net mobilized sediment volumes (V) increased again during phases of fan incision (i.e., DS and IW phases of Fig. 7c and d) and main-channel incision (e.g., IW phase in Fig. 7f). These increases were due to the combined effect of a general increase in sediment mobility within the active valley floor (V_{vf}) and lateral erosion of the banks (V_b) (Fig. 7, violet and orange bars respectively, and Fig. S8 of the Supp. Material). The DoD analysis also indicates that in all experiments, with the only exception of the MC run and of the phases approaching steady-state, bank contribution was higher or of the same order of magnitude of the volume mobilized in the valley floor (Fig. 7, orange and violet bars). This observation suggests that bank erosion represented a major contribution to Q_{s_out} (Tables S3 to S8 of Supp. Material) and is particularly

true for the T_NC2 run, where aggradation was favored, in which Q_{s_out} is dominated by the contribution of the banks (Fig. 7e, and Fig. S9 of the Supp. Material).

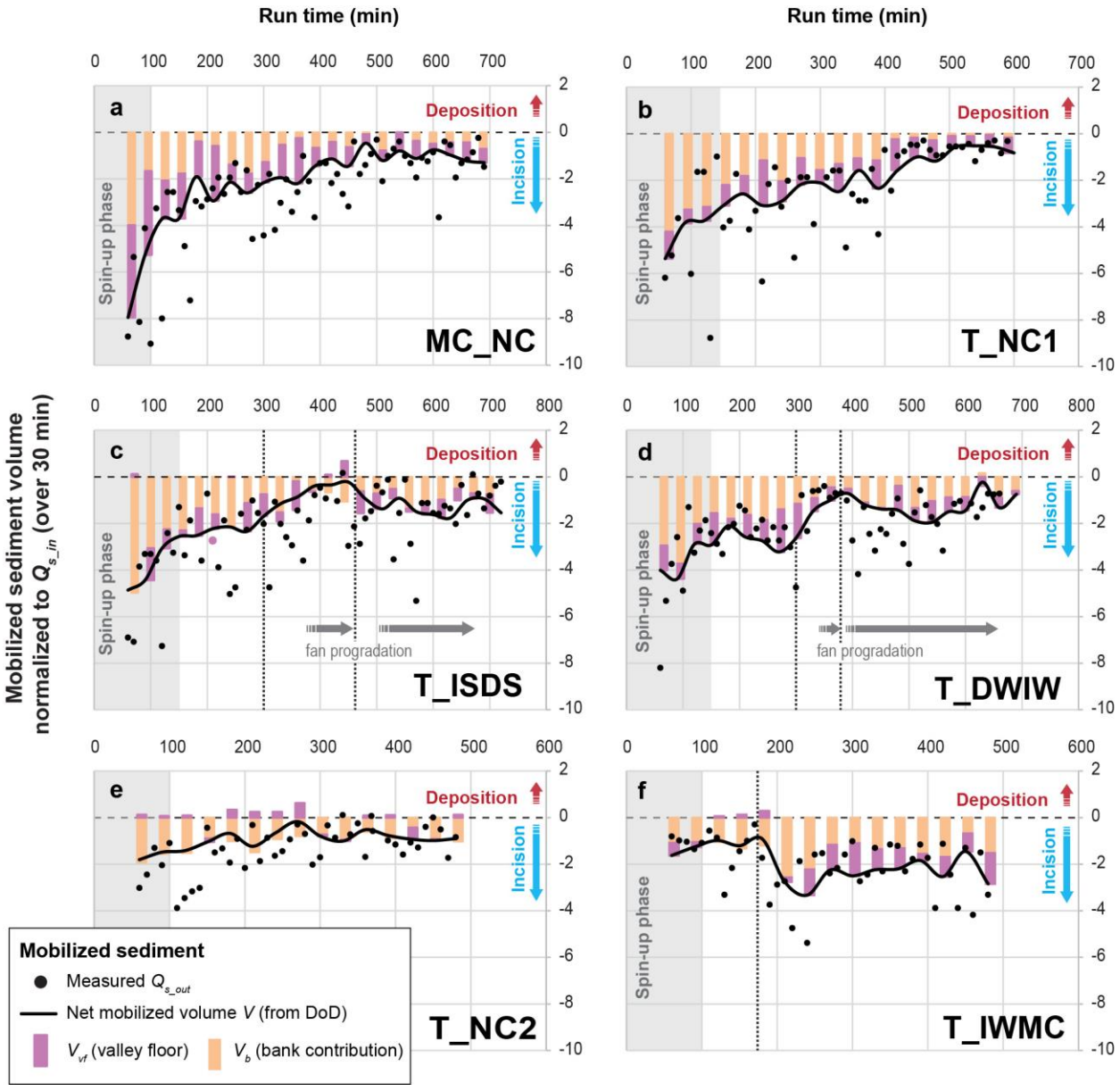

Figure 7. Volumes of sediment mobilized within the system. Black line: Net mobilized volume of sediment measured using the DoD. For comparison, black dots represent the Q_{s_out} values measured every 10 minutes (part of the difference between measured and calculated Q_{s_out} values may be due to the contribution of the most downstream area of the wooden box, which was shielded in the DEM reconstruction). Horizontal arrows indicate the timespan of fan progradation either during fan aggradation or fan incision. Vertical pointed lines represent the *time of change* in boundary conditions; horizontal dashed line separates aggradation and erosion.

4.3. Downstream sediment propagation

To analyze the effects of the tributary on the mobility of sediment within the coupled tributary–main-channel system, we monitored the volumes of sediment mobilized (V) in the upper, middle, and lower sections of the fluvial network through time (Fig. 8). The complex pattern of V in the different sections yields insights into downstream sediment propagation, especially when coupled with maps of the spatial distribution of eroded and deposited sediment (Figs. S2 to S7 in the Supp. Material):

1. In all experiments, including the one without a tributary (MC_NC), sediment moved in pulses through the system (Fig. 8). As such, the mobilized volumes (V) of each section can be *in-phase* or *out-of-phase* with the volumes mobilized in the others sections (Castelltort and Van Den Driessche, 2003) depending on where the "pulse" of sediment was located within the floodplain (Fig. 9a).
2. The sediment mobilized in the middle and lower sections of the T_NC1 run showed a decrease in V after ca. 400 min, whereas in the upper section V remained nearly constant (Fig. 8b), despite a marked increase in V_{vf} (Fig. S8 of Supp. Material).
3. In the T_ISDS run, the middle section showed, as expected, a strong reduction in V after the onset of increased Q_{s_in} in the tributary and consequent fan aggradation (300 to 480 minutes). Conversely, it showed an increase in V following the decrease in Q_{s_in} and consequent fan incision (480 minutes to the end of the run) (Fig. 8c). A similar pattern can be seen in the lower section, with a reduction in V during fan aggradation and an increase in V during fan incision. Interestingly, the upper section showed two peaks of enhanced V (i.e., increase in sediment export) just after the changes in the tributary, followed by a prolonged reduction of V (i.e., decrease in sediment export) during phases of fan progradation.
4. Patterns similar to those described for the T_ISDS can be seen for the T_DWIW run. However, due to the type of change in the tributary (i.e., decrease in Q_w, which increases the Q_s/Q_w ratio, reducing the sediment-transport capacity) and due to the shorter duration of the perturbation (300 to 375 minutes), the first peak of enhanced V in the upper section was barely visible, whereas the second peak was not present. Rather, the upper

section shows a continuous decrease in V until ca. 420 min, i.e., circa 45 minutes after the onset of increased Q_w in the tributary (Fig. 8d and Fig. S5 of Supp. Material).

5. The T_NC2 experiment is dominated by aggradation and V values are rather constant; (Fig. 8e and Fig. S6 of Supp. Material). Similar to the final part of the T_NC1 run, the upper section of the main channel showed a general increasing trend in V_{vf} (Fig. S9 of Supp. Material).
6. In the T_IWMC experiment, as expected, V increased immediately after the increase in Q_w in main channel in all three sections (indicating major incision), but was particularly evident in the upper and lower sections of the main channel (Fig. 8f).

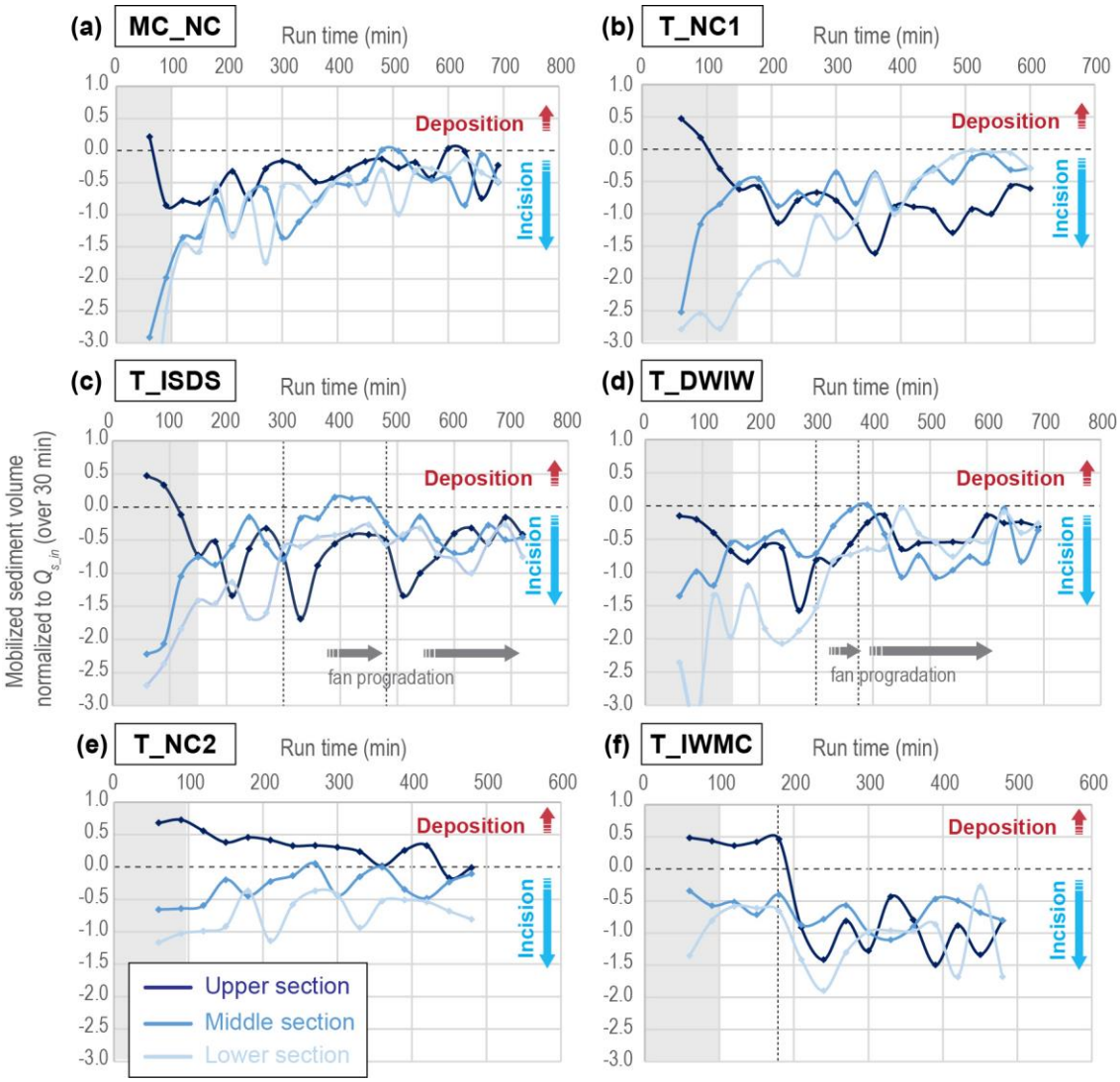

Figure 8. Volume (V) of sediment mobilized in each section (e.g., upper, middle, and lower sections). Vertical lines represent the *times of change* in boundary conditions; horizontal dashed line separates aggradation and erosion.

5. Discussion

Our six experiments provide a conceptual framework for better understanding how tributaries interact with main channels under different environmental forcing conditions (Fig. 1). We particularly considered geometric variations of the two subsystems (i.e., tributaries and main channels) and the effects of tributaries on the downstream delivery of sediment within the fluvial system.

5.1. Aggrading and incising fans: geometrical adjustments and tributary–main-channel interactions

In our experiments, the aggrading alluvial fans strongly impacted the width of the main-channel valley both upstream and downstream of the tributary junction. By forcing the main channel to flow against the valley-wall opposite the tributary, bank erosion was enhanced (Tables S3 to S8 and Fig. S8 in the Supp. Material), thus widening the main-channel valley floor (Figs. 4, 6, and S4). Bank erosion and valley widening in the main channel also occurred during periods of fan incision (Figs. S4b, S5, and S8 of the Supp. Material). We hypothesize that this widening was related to pulses of sediment eroded from the fan, which periodically increased the sediment load to the main channel and helped to push the river to the side opposite the tributary (Grimaud et al., 2017; Leeder and Mack, 2001). Once there, the river undercut the banks, causing instability and collapse. As such, periods of fan incision triggered a positive feedback between increased load in the main channel and valley widening, which occurred through bank erosion and bank collapses. In these scenarios, bank contribution (V_b) in the middle and lower sections of the main channel can be equal to, or larger than, the sediment mobilized within the active valley floor (V_{vf}) (also for the T_NC2 run; Fig. 7b and Fig. S8 and S9, Supp. Material). It follows that the composition of the fluvial sediment may be largely dominated by material mobilized from the valley walls, with important consequences, for example, for geochemical or provenance studies (Belmont et al., 2011).

Our analysis of sediment mobility within the different sections of the main channel highlighted that the presence of the alluvial fan affects the time needed to reach equilibrium in the different reaches of the main river: in the T_NC1 run, for example, due to the sediment input from the tributary, the middle and lower sections have a higher Q_s/Q_w ratio (0.022) than the upper section (0.014), and may reach equilibrium faster (Gilbert, 1877; Wickert and Schildgen, 2019). Once the tributary channel-profile reached equilibrium (e.g., at ca. 420 minutes for T_NC1; inset of Fig. 4b), the upper main channel rapidly adjusted by decreasing the elevation of its channel bed (Fig. 4b) and increasing the sediment mobilized (Fig. 8b and Fig. S8 of Supp. Material). This result suggests that equilibrium time scales of channels upstream and downstream of tributaries can vary (Schumm, 1973), and that in a top-down direction of adjustments, the equilibrium state of the upper section may be dictated by the equilibrium state of its lower reaches because of the tributary influence.

In our experiments, fans were built under conditions that caused deposition at the tributary junction (e.g., an increase in Q_{s_in} or decrease in Q_w in the tributary). When the perturbation lasted long enough (e.g. in experiment T_ISDS), the fan prograded into the main channel. The passage from fan aggradation to progradation was delayed relative to the onset of the perturbation by the time necessary to move the sediment from the fan head to the fan margin (e.g. for > 60 min in T_ISDS; Fig. S4b). This delay allowed for a temporarily efficient transfer of sediment within the main channel (as marked by the peak in V of the upper main channel section; Fig. 8c). For tributaries subject to a change that caused tributary incision (e.g., decrease in Q_{s_in} or increase in Q_w), the elevation of the fan surface was progressively lowered (inset of Fig. 4c and d, and Fig. S1 in the Supp. Material), and the fan prograded into the main channel with cyclic pulses of sediment discharge (e.g., Fig. S4c) (Kim and Jerolmack, 2008). Progradation was generally localized where the tributary channel debouched into the main river (e.g., depositing the *healing wedge* of Leeder and Mack, 2001), generally shortly after (< 30 min) the onset of the perturbation (Figs. S4c and S5 of the Supp. Material). When the fan prograded, sediment in the main channel was partially blocked above the tributary junction (e.g., at 390 to 480 min in Fig. S4b, and at 510 min to the end of the run in Fig. S4c; Fig. S6 of Supp. Material), and the upstream main-channel section experienced a prolonged decrease in sediment mobility due to localized aggradation (Fig. 8c and d, and Fig. 9b).

Given the relative size of the tributary and main channel in our experiments (Q_w tributary ~ 2/3 Q_w main channel) and the magnitude of the perturbations (doubling of Q_{s_in} or halving of Q_w), the impact of perturbations in the tributary on the sediment mobility (V) within the main channel remained mostly within autogenic variability (Fig. 7b, Group 1). This observation highlights how the analysis of changes in Q_{s_out} alone (for example inferred from the stratigraphy of a fluvial deposit) may not directly reflect changes that occurred in the tributary, but can be overprinted by autogenic variability. However, the analysis of V within individual sections of the main channel, and particularly within the confluence zone (i.e., middle section), together with the analysis of how sediment moves in space, reveal important changes in the sediment dynamics of the main channel that may help to reconstruct the perturbations that affected the tributary (Section 5.2; Figs. 8 and 9b). This observation underscores the need to study a range of sedimentary deposits of both the tributary and main-channel (Mather et al., 2017), both upstream and downstream of a tributary junction.

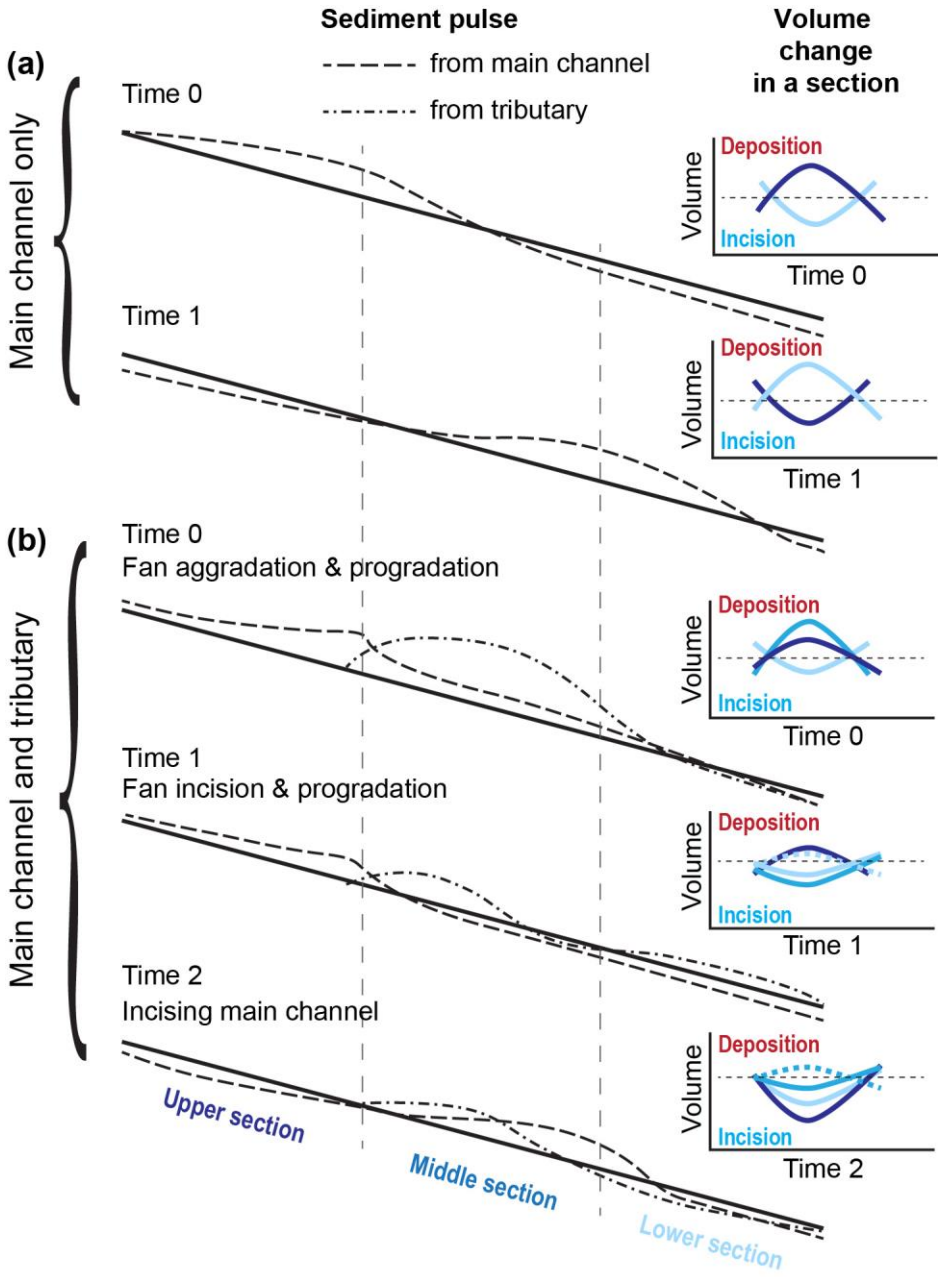

522

523 Figure 9. Schematic representation of the average sediment mobilized in each section of the main
524 channel. Solid black line represents the idealized equilibrium profile of the main channel,
525 whereas dashed lines represent the volumes mobilized from the main channel and from the
526 tributary. (a) Sediment dynamics in a single-channel system: sediment moves in pulses and upper
527 and lower sections may be *out-of-phase* or *in-phase* depending on the dynamics of the middle
528 section (i.e., the *transfer zone* of Castelltort and Van Den Driessche, 2003). (b) Sediment
529 dynamics in a tributary-main channel system: *Time 0* represents the "aggrading (and prograding)
530 fan" scenario, where the upper and middle sections of the main channel undergo aggradation,
531 while the lower section undergoes incision. *Time 1* represents the "incising (and prograding) fan"
532 scenario, where the upper section may still be aggrading by it also starts to get incise creating a
533 pulse of sediment that reaches the lower section. The middle section clearly sees an increase in

incision due to the imposed perturbation, while the lower section may undergo incision or aggradation depending on the amount of sediment delivered from the fan, from the upper section, and from bank erosion. *Time 2* represents the "incising main channel" scenario, where the fan loses its influence on the dynamics of the main channel and both upper and lower sections undergo incision. The middle section can undergo aggradation or incision depending on the amount of sediment mobilized in the tributary and on the pulse of sediment moving from the upper to the lower section of the main channel.

5.2. Incising main channel: geometric adjustments and tributary–main-channel interactions

The main-channel bed elevation dictates the local base level of the tributary, such that variations in the main-channel long profile may cause aggradation or incision in the tributary (Cohen and Brierly, 2000; Leeder and Mack, 2001; Mather et al., 2017). In our experiments, lowering of the main-channel bed triggered tributary incision that started at the fan toe and propagated upstream (insets in Fig. 4). Because tributary incision increases the volume of sediment supplied to the main channel, a phase of fan progradation would be expected, similar to the cases described above (and in the *complex response* of Schumm, 1973). However, in our experiment (i.e., T_IWMC), progradation did not occur: instead, the fan was shortened (Fig. S7 Supp. Material). We hypothesize that the increased transport capacity of the main river resulted in an efficient removal of the additional sediment from the tributary, thereby mitigating the impact of the increased sediment load supplied by the tributary to the main channel. Another consequence is that the healing wedge of sediment from the tributary is likely not preserved in the deposits of either the fan margin or the confluence zone, hindering the possibility to reconstruct the changes affecting the tributary. However, some insight can be obtained from the analysis of sediment mobility. During main-channel incision, whereas both upper and lower sections of the main channel registered a marked increase in V following the perturbation, the middle section showed only minor variations (Fig. 8f). We hypothesize that this lower variability was due to the buffering effect of the increased load supplied from the fan undergoing incision (i.e., caused by the sudden base-level fall that followed main-channel incision) (Fig. 9b). In contrast, when incision in the tributary was caused by a perturbation in its headwaters, V initially increased and then showed a prolonged decrease in the upper section during fan aggradation, whereas it increased in the middle section during fan incision. These differences may help to

discern the cause of fan incision (i.e., either a perturbation in the main channel or in the tributary).

We did not observe the *complex response* described by Schumm (1973), characterized by tributary aggradation following incision along the main channel. The complex response in Schumm's experiments likely occurred because the main river had insufficient power to remove the sediment supplied by the tributaries, as opposed to what occurred in our experiments. When aggradation occurs at the tributary junction, one may expect to temporarily see an evolution similar to that proposed in the "aggrading alluvial fan" scenario, with the development on an alluvial fan that may alter the sediment dynamics of the main channel, modulating the sediment mobilized in the upper and lower sections of the river and delaying main-channel adjustments. In our experiment, instead, a prolonged erosional regime within the main channel may have led to fan entrenchment and fan-surface abandonment (Clarke et al., 2008; Nicholas and Quine, 2007; Pepin et al., 2010; Van Dijk et al., 2012). Despite the lack of fan progradation, an increase in bank contribution following incision of the main channel did occur (Fig. 7b.6, Fig. S9 Supp. Material) and could be explained by (1) higher and more unstable banks and (2) an increased capacity of the main channel to laterally rework sediment volumes under higher water discharges (Bufe et al., 2019).

5.3. Sediment propagation and coupling conditions

Understanding the interactions between tributaries and main channel, and the contribution of these two sub-system to the sediment moved (either eroded or deposited) in the fluvial system, is extremely important for a correct interpretation of fluvial deposits (e.g., cut-and-fill terraces or alluvial fans), which are often used to reconstruct the climatic or tectonic history of a certain region (e.g., Armitage et al., 2011; Densmore et al., 2007; Rohais et al., 2012; Simpson and Castelltort, 2012).

In their conceptual model, Mather et al. (2017) indicate that an alluvial fan may act as a *buffer* for sediment derived from hillslopes during times of fan aggradation, and as a *coupler* during times of fan incision, thereby allowing the tributary's sedimentary signals to be transmitted to the main channel. From our experiments, we can explore the effects that tributaries have not only in storing or releasing sediment to the main channel, but also in modulating the flux of sediment within the fluvial system. In doing so, we create a new conceptual framework

596 that takes into account the connectivity within a coupled alluvial fan-main channel system and
597 the mechanisms with which sediment and sedimentary signals may be recorded in local deposits
598 (Fig. 10). Results are summarized as follows.

599 *5.3.1. Aggrading and incising fans*

600 1. If the tributary has perennial water discharge, a *partial coupling* between the tributary
601 and the main channel is possible. Also, during fan aggradation, when most of the
602 sediment is deposited and stored within the fan (e.g., Fig. S4b), a portion of the Q_{s_in}
603 reaches the main channel in proportion to the transport capacity of the tributary channel
604 (Fig. 10a and b). The partial coupling between the fan and the main channel allows for a
605 *complete coupling* between the upstream and downstream sections of the main river (Fig.
606 S4b – 300-390 min, and S5b in the Supp. Material). As such, during fan aggradation, the
607 main channel behaves as a single connected segment, and the lower section receives
608 sediment in proportion to the transport capacity of the main and tributary channels. The
609 material supplied by the tributary to the main channel is dominated by the tributary's
610 Q_{s_in} with little remobilization of previously deposited material.
611 2. During fan incision, large volumes of sediment are eroded from the fan and transported
612 into the main channel as healing wedges, allowing the fan to prograde into the main
613 channel (Fig. S4c and 10c). This process creates a *complete coupling* between the
614 tributary and the main channel (Fig. 8c and d), with the material supplied by the tributary
615 mostly dominated by sediment previously deposited within the fan.
616 3. During times of fan progradation, the fan creates an obstacle to the transfer of sediment
617 down the main channel, creating a *partial decoupling* between upstream and downstream
618 sections of the main channel (Fig. 8, S4b and c, and 10b and c). As a consequence, the
619 sediment carried by the main channel is trapped above the tributary junction and thus will
620 be missing from downstream sedimentary deposits. However, the upstream section of the
621 main channel may be periodically subject to incision (e.g., Fig. S4b and c), moving
622 mobilized sediment from the upper to the lower section. Accordingly, if progradation of
623 the fan is caused by prolonged fan aggradation, the downstream section will receive the
624 Q_{s_in} from the fan, plus pulses of sediment eroded from the upstream section of the main
625 channel. Conversely, if progradation is due to incision of the tributary and mobilization
626 of additional fan sediment, the downstream section will receive pulses of erosion from

either the fan or the upstream section of the main channel, plus the contribution of bank erosion.

In summary, downstream fluvial deposits record the competition between the main channel and the tributary: the alluvial fan pushes the main channel towards the opposite side of the valley to adjust its length, whereas the main channel tries to maintain a straight course by removing the material deposited from the fan. If the main channel dominates, it cuts the fan toe and permits sediment from upstream of the junction to be more easily moved downstream. If the tributary dominates, the main channel will be displaced and the transfer of sediment through the junction will be disrupted. An autogenic alternation of these two situations is possible, whereby fan-toe cutting may trigger fan incision and progradation, increasing the influence of the fan on the main channel. The composition of the sediment downstream thus reflects the competition between main channel and alluvial fan, with contributions from both sub-catchments. In addition, bank erosion may make important contributions to sediment supply and transport, particularly during periods of fan incision (Fig. S8 in the Supp. Material). From these results, we therefore distinguish between: 1) *Influential alluvial fans*, which have a strong impact on the geometry and sediment-transfer dynamics of the main channel, and 2) *Non-influential alluvial fans*, which do not substantially alter the geometry or sediment-transfer dynamics of the main channel.

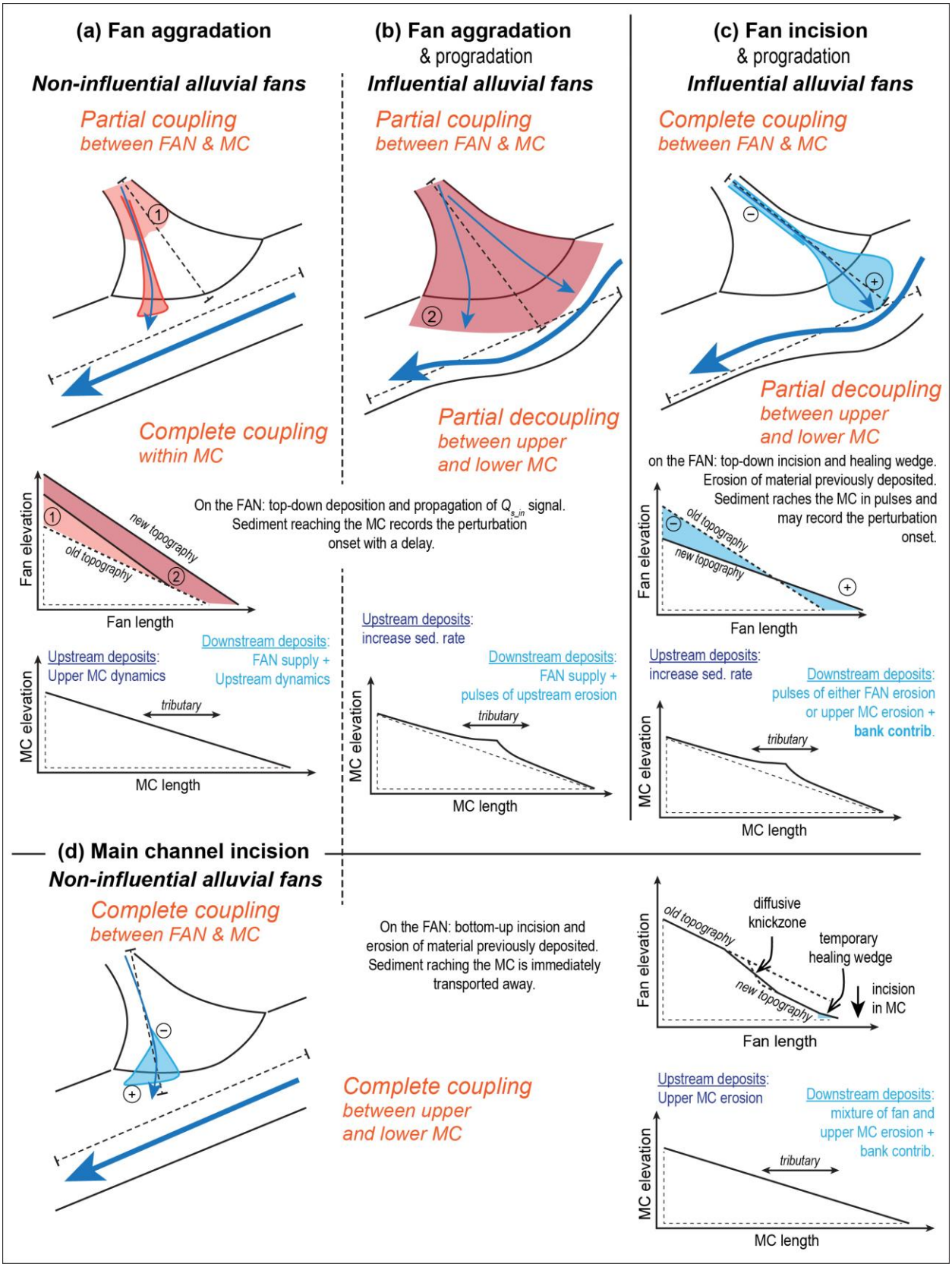
(a) Fan aggradation
Non-influential alluvial fans
Partial coupling
between FAN & MC
Complete coupling
within MC
(b) Fan aggradation
& progradation
Influential alluvial fans
Partial coupling
between FAN & MC
Partial decoupling
between upper
and lower MC
(c) Fan incision
& progradation
Influential alluvial fans
Complete coupling
between FAN & MC
Partial decoupling
between upper
and lower MC
On the FAN: top-down deposition and propagation of Q_{s_in} signal.
Sediment reaching the MC records the perturbation
onset with a delay.
on the FAN: top-down incision and healing wedge.
Erosion of material previously deposited.
Sediment raches the MC in pulses and
may record the perturbation
onset.
Fan elevation
Fan length
new topography
old topography
Upstream deposits:
Upper MC dynamics
Downstream deposits:
FAN supply +
Upstream dynamics
Upstream deposits:
increase sed. rate
Downstream deposits:
FAN supply +
pulses of upstream erosion
Upstream deposits:
increase sed. rate
Downstream deposits:
pulses of either FAN erosion
or upper MC erosion +
bank contrib.
MC elevation
MC length
tributary
(d) Main channel incision
Non-influential alluvial fans
Complete coupling
between FAN & MC
On the FAN: bottom-up incision and
erosion of material previously deposited.
Sediment raching the MC is immediately
transported away.
Complete coupling
between upper
and lower MC
diffusive
knickzone
temporary
healing wedge
incision
in MC
Upstream deposits:
Upper MC erosion
Downstream deposits:
mixture of fan and
upper MC erosion +
bank contrib.

646

Figure 10. Conceptual framework for the coupling conditions of an alluvial-fan/main-channel (*MC*) system under different environmental forcings. For *aggrading and incising alluvial fans* (upper panels), the fan-main channel connectivity depends on the dynamics acting in the alluvial fan, being partially coupled during fan aggradation and totally coupled during fan incision. For *incising main rivers* (lower panel) the fan and main channel are fully coupled. As well, *non-influential alluvial fans* (left and lower panels) favors a complete coupling within the main channel, whereas *influential alluvial fans* (middle and right upper panels) may favor a partial decoupling between upstream and downstream sections of the main river. Each one of the four settings presented here brings its own sedimentary signature, different responses to perturbations, and dynamics of signal propagation which may be recorded into the fluvial deposits.

5.3.2. Incising main channel

1. Lowering of the main-channel bed triggers incision into the alluvial fan, thereby promoting a *complete coupling* between the fan and the main channel (Fig. 10d, and S7 in the Supp. Material). The sediment supplied by the tributary is mainly composed of material previously deposited within the fan.
2. An increase in main-channel water discharge increases the transport capacity of the mainstem so that it persistently "wins" the competition with the alluvial fan. In this case, despite the incision triggered in the alluvial fan, which increases the sediment supplied by the tributary, the main channel efficiently removes the additional sediment load, thereby reducing the influence of the alluvial fan on downstream sediment transport within the main channel (Fig. S7 in the Supp. Material). The consequence is a *complete coupling* between the upstream and downstream sections of the main channel (Fig. 10d). The sediment reaching the lower section is a mixture of eroded material from the main channel, within the fan, and along the banks.

5.4. Limitations of the experiments and implications for field studies

Physical experiments have the advantage of simulating many of the complexities of natural systems in a simplified setting (Paola et al., 2009). Because of the simplifications, however, a number of limitations arise when attempting to compare experimental results to natural environments. One limitation of our study concerns the small number of experiments that we have performed compared to the full variability of natural river systems and the lack of repetition of experiments. This limitation prevents us, for example, from fully distinguishing significant trends in sediment mobility from stochastic or autogenic processes that are inherent of alluvial

systems. In Section 2.2, we described how fan-toe cutting may create the same response in the tributary as incision along the main channel. However, we are not able to quantify the relative contribution of these two processes on the changes occurring in the tributary. One way to distinguish between fan-toe cutting and main-channel incision is to study the whole fluvial system, thus including all tributaries: Main channel variations will affect all tributaries with a timing that is diachronous in the direction of the change (Mather et al., 2017 and references therein). Fan-toe cutting, on the other hand, will be specific of single tributaries with "random" timings.

Another limitation of our experiments relates to the *scaling*. Our experiments were not scaled to any particular environment. Instead we used the principle of *similarity of processes* as suggested by Hooke (1968). However, the use of a single grain size for both the tributary and the main channel prevents us from analyzing geomorphic changes that are associated to the input of a coarser grain size from a tributary or to the thinning of sediment in the main channel upstream of the fan. In this regard, we point again to the work of Ferguson et al. (2006) which, by analyzing the effects of grain-size variations on channel slope, may represent a good complement to our analyses. Finally, the patterns highlighted by our experiments are partially dictated by the choices made in setting the values of Q_w and Q_{s_in}, and by the timing and the magnitude of the imposed perturbations.

Despite these shortcomings, the analysis presented here provides insights into how channels respond to changes in water and sediment discharge at confluence zones, and how sediment moves through branched fluvial systems. In particular, the dynamics that govern the movement of sediment can have important repercussions for field studies, particularly for interpretations of alluvial-channel long profiles, dating of material within stratigraphic sequences, and for interpretations of their geochemical composition (e.g., Tofelde et al., 2019, and references therein). Additionally, by partially decoupling the upper and lower sections of the main channel, fan progradation may lead to pulses of sediment movement from the upper to the lower sections of the main channel, therefore disrupting environmental signals that could be transmitted downstream (e.g., Simpson and Castelltort, 2012). Indeed, the stratigraphy of the downstream section of the main channel may record periods of high sedimentation rates, erroneously pointing

to periods of high sediment supply, when in reality the fast accumulation may be related to a pulse of sediment being eroded from the upstream section of the main channel.

These complexities highlight the need for further research on these topics and the importance of studying the coupled tributary-main channel system to fully understand the dynamics acting in the river network and correctly interpret both geochemical and stratigraphic signals.

6. Conclusion

We performed six experiments to analyze the interactions of a tributary–main-channel system when a tributary produces an alluvial fan. We found that differing degrees of coupling may be responsible for substantial changes in the geometry of the main channel and the sediment transfer dynamics of the system. In general, we found that the channel geometry (i.e., channel slope and valley width) adjusts to changes in sediment and water discharge in accordance with theoretical models (e.g., Ferguson and Hoey, 2008; Parker et al., 1998; Whipple et al., 1998; Wickert and Schildgen, 2019). Additionally, by analyzing the effects of the tributary-main channel interactions on the downstream delivery of sediment, we have shown that the fluvial deposits within the main channel above and below the tributary junction may record perturbations to the environmental conditions that govern the fluvial system.

Our main results can be summarized as follows (Fig. 10):

(1) Fan aggradation leads to a partial coupling between the fan and the main channel, which permits a complete coupling between the main-channel reaches upstream and downstream of the tributary junction. As such, the provenance of downstream sediment reflects the dynamics of both sub-catchments (e.g., tributary and main river), and remobilized material from older deposits will be minimal.

(2) Fan incision favors a complete coupling between the fan and the main channel, and remobilizes material previously stored in the fan.

(3) Fan progradation (either during prolonged aggradation or fan incision) strongly influences the main channel. As a result, the connectivity of the main river across the tributary junction is reduced and the deposits of the fluvial system above and below the junction may record different processes.

(4) Incision along the main channel triggers incision in the alluvial fan that, despite an increased sediment supply to the main river, reduces its influence on the dynamics of the main channel. The result is a fully connected fluvial system in which the deposits record sediment-transfer dynamics and the interactions between both the alluvial fan and the main river, including a large component of material remobilized from older deposits.

The theoretical framework proposed in this study aims to illustrate the dynamics acting within a tributary junction. It provides a first-order analysis of how tributaries affect the sediment delivered to the main channels and of how sediment is moved through the system under different environmental forcing conditions. The (dis)connectivity within the fluvial system has important consequences for the stratigraphy and architecture of depositional sinks, as it may be responsible for the continuity of the sedimentary record or for the disruption of the environmental signals carried through the main channel (Simpson and Castelltort, 2012). Our findings may be used to improve the understanding of the interactions between tributaries and main channels, providing essential information for the reconstruction of the climatic or tectonic histories of a basin.

Data availability

Data, DEMs and videos are available through the Sediment Experimentalists Network Project Space to the SEAD Internal Repository (https://sead2.ncsa.illinois.edu/spaces/5e7635f6e4b05435defb5b63).

Video supplement

Time-lapse video of the experiment will be uploaded.

Supplement

Supplement tables and figures can be found in the supplementary document.

Author contributions

SS, ST, and ADW designed and built the experimental setup. SS and ST performed the experiments. SS analyzed the data with the help of ST, ADW and AB. All authors discussed the data, designed the manuscript, and commented on it. SS designed the artwork.

Competing interests

The authors declare that they have no conflict of interest.

Acknowledgments

We thank Ben Erickson, Richard Christopher, Chris Ellis, Jim Mullin, and Eric Steen for their help in building the experimental setup and installing equipment. We are also thankful to Jean-Louis Grimaud and Chris Paola for fruitful discussions and suggestions.

Financial support

This research has been supported by the Deutsche Forschungsgemeinschaft (grant no. SCHI 1241/1-1 and grant no. SA 3360/2-1), the Alexander von Humboldt-Stiftung (grant no. ITA 1154030 STP), and the University of Minnesota**.**

References

778 Allen, P. A.: From landscapes into geological history, Nature, 451, 274–276,
779 https://doi.org/10.1038/nature06586, 2008.
780
781 Armitage, J. J., Duller, R. A., Whittaker, A. C., and Allen, P. A.: Transformation of tectonic
782 and climatic signals from source to sedimentary archive, Nat. Geosci., 4, 231–235, 2011.
783
784 Belmont, P., Gran, K.B., Schottler, S.P., Wilcock, P.R., Day, S.S., Jennings, C., Lauer, J.W.,
785 Viparelli, E., Willenbring, J.K., Engstrom, D.R., and Parker, G.: Large Shift in Source of Fine
786 Sediment in the Upper Mississippi River. Environmental Science and Technology, 45, 8804–
787 8810, 2011.
788
789 Benda, L.: Confluence environments at the scale of river networks. In: River Confluences,
790 Tributaries and the Fluvial Network © John Wiley & Sons, Ltd. ISBN: 978-0-470-02672-4,
791 2008.
792
793 Benda, L., Miller, D., Bigelow, P., and Andras, K.: Effects of post-wildfire erosion on
794 channel environments, Boise River, Idaho. Forest Ecology and Management, v. 178, 105–119,
795 doi:10.1016/S0378-1127(03)00056-2, 2003.
796
797 Benda, L., Leroy Poff, N., Miller, D., Dunne, T., Reeves, G., Pess, G., and Pollock, M.: The
798 Network Dynamics Hypothesis: How Channel Networks Structure Riverine Habitats.
799 BioScience, v. 54(5), 413-427, 2004a.
800
801 Benda, L., Andras, K., Miller, D., and Bigelow, P.: Confluence effects in rivers: Interactions
802 of basin scale, network geometry, and disturbance regime. Water Resources Research, 40,
803 W05402, doi:10.1029/2003WR002583, 2004b.
804
805 Best, J.L.: The morphology of river channel confluences. Progress in Physical Geography:
806 Earth and Environment, v. 10(2), 157-174, https://doi.org/10.1177/030913338601000201, 1986.
807
808 Best, J.L.: Sediment transport and bed morphology at river channel confluences.
809 Sedimentology, 35,481-498, 1988.
810
811 Best, J.L., and Rhoads B.L.: Sediment transport, bed morphology and the sedimentology of
812 river channel
813 Confluences. In: River Confluences, Tributaries and the Fluvial Network © John Wiley &
814 Sons, Ltd. ISBN: 978-0-470-02672-4, 2008.
815
816 Bierman, P. and Steig, E. J.: Estimating rates of denudation using cosmogenic isotope
817 abundances in sediment, Earth Surf. Proc. Land., 21, 125–139,
818 https://doi.org/10.1002/(SICI)1096-9837(199602)21:2<125::AID-ESP511>3.0.CO;2-8, 1996.
819
820 Brown, E. T., Stallard, R. F., Larsen, M. C., Raisbeck, G. M., and Yiou, F.: Denudation rates
821 determined from the accumulation of in situ-produced 10Be in the Luquillo Experimental Forest,
822 Puerto Rico, Earth Planet. Sc. Lett., 129, 193–202, https://doi.org/10.1016/0012-
823 821X(94)00249-X, 1995.

Bryant M., Falk P., and Paola C.: Experimental study of avulsion frequency and rate of deposition. Geology; v. 23; no. 4; 365–368, 1995.

Bufe, A., Turowski, J.M., Burbank, D.W., Paola, C., Wickert, A.D., and Tofelde, S.: Controls on the lateral channel migration rate of braided channel systems in coarse non-cohesive sediment. Earth Surface Processes and Landforms, https://doi.org/10.1002/esp.4710, 2019.

Bull W.B.: Threshold of critical power in streams. Geological Society of America Bulletin, Part I, v. 90, 453-464, 1979.

Castelltort S., and Van Den Driessche J.: How plausible are high-frequency sediment supply-driven cycles in the stratigraphic record? Sedimentary Geology, v. 157, 3 –13; doi:10.1016/S0037-0738(03)00066-6, 2003.

Clarke L. E., Quine T.A., and Nicholas A.P.: Sediment Dynamics in Changing Environments (Proceedings of a symposium held in Christchurch, New Zealand, December 2008). IAHS Publ. 325, 2008.

Clarke L. E., Quine T.A., and Nicholas A.P.: An experimental investigation of autogenic behaviour during alluvial fan evolution. Geomorphology, v. 115, 278–285; doi:10.1016/j.geomorph.2009.06.033, 2010.

Cohen, T.J., and Brierley, G.J.: Channel instability in a forested catchment: a case study from Jones Creek, East Gippsland, Australia. Geomorphology, 32, 109–128, 2000.

D'Arcy, M., Roda-Boluda, D.C., Whittaker, A.C.: Glacial-interglacial climate changes recorded by debris flow fan deposits, Owens Valley, California. Quaternary Science Reviews, 169, 288-311, 2017.

Dingle, E. H., Attal, M., and Sinclair, H. D.: Abrasion-set limits on Himalayan gravel flux, Nature, 544, 471–474, 5 https://doi.org/10.1038/nature22039, 2017.

De Haas T., Van den Berg W., Braat L., and Kleinhans M.G.: Autogenic avulsion, channelization and backfilling dynamics of debris-flow fans. Sedimentology, v. 63, 1596–1619. Doi; 10.1111/sed.12275, 2016.

Densmore A.L., Allen P.A., and Simpson G.: Development and response of a coupled catchment fan system under changing tectonic and climatic forcing. J. Geophys. Res., 112, F01002, doi:10.1029/2006JF000474, 2007

Faulkner, D.J., Larson, P.H., Jol, H.M., Running, G.L., Loope, H.M., and Goble, R.J.: Autogenic incision and terrace formation resulting from abrupt late-glacial base-level fall, lower Chippewa River, Wisconsin, USA. Geomorphology, v. 266, 75–95, http://dx.doi.org/10.1016/j.geomorph.2016.04.016, 2016.

Ferguson, R.I., Cudden, J.R., Hoey, T.B., and Rice, S.P.: River system discontinuities due to lateral inputs: generic styles and controls. Earth Surf. Process. Landforms, v. 31, 1149–1166, doi: 10.1002/esp.1309, 2006.

Ferguson, R.I., and Hoey, T.: Effects of tributaries on main-channel geomorphology. In: River Confluences, Tributaries and the Fluvial Network © John Wiley & Sons, Ltd. ISBN: 978-0-470-02672-4, 2008.

Gao L., Wang X., Yi S., Vandenberghe J., Gibling M.R., and Lu H.: Episodic Sedimentary Evolution of an Alluvial Fan (Huangshui Catchment, NE Tibetan Plateau). Quaternary, v. 1(16); doi:10.3390/quat1020016, 2018.

Germanoski, D., Ritter, D.F.: Tributary response to local base level lowering below a dam. Regulated rivers: research and management, v. 2, 11-24, 1988.

Gilbert, G. K.: Report on the Geology of the Henry Mountains, US Gov. Print. Off., Washington, D.C., USA, https://doi.org/10.3133/70038096, 1877.

Giles P.T., Whitehouse B.M., and Karymbalis E.: Interactions between alluvial fans and axial rivers in
Yukon, Canada and Alaska, USA. From: Ventra, D. & Clarke, L. E. (eds) Geology and Geomorphology of Alluvial and Fluvial Fans: Terrestrial and Planetary Perspectives. Geological Society, London, Special Publications, v. 440; http://doi.org/10.1144/SP440.3, 2016.

Gippel, C.: Changes in stream channel morphology at tributary junctions, Lower Hunter Valley,
New South Wales. Australion GeOgfQphiCQl Studies, v. 23, 291-307, 1985.

Grant, G.E., and Swanson, F.J.: Morphology and Processes of Valley Floors in Mountain Streams,
Western Cascades, Oregon. Natural and Anthropogenic Influence in Fluvial Geomorphology, Geophysical Monograph, 89, 1995.

Granger, D. E., Kirchner, J. W., and Finkel, R.: Spatially averaged long-term erosion rates measured from in situ-produced cosmogenic nuclides in alluvial sediment, J. Geol., 104, 249–257, 1996.

Heine, R.A., and Lant, C.L.: Spatial and Temporal Patterns of Stream Channel Incision in the Loess Region of the Missouri River, Annals of the Association of American Geographers, 99(2), 231-253, DOI: 10.1080/00045600802685903, 2009.

Hamilton P.B., Strom K., and Hoyal D.C.J.D.: Autogenic incision-backfilling cycles and lobe formation during the growth of alluvial fans with supercritical distributaries. Sedimentology, v, 60, 1498–1525; doi: 10.1111/sed.12046, 2013.

Hooke R.L.: Model Geology: Prototype and Laboratory Streams: Discussion. Geological Society of America Bulletin, v. 79, 391-394, 1968.

Hooke R.L., and Rohrer W.L.: Geometry of alluvial fans: effect of discharge and sediment size. Earth Surface Processes, v. 4, 147-166, 1979.

Kim W., and Jerolmack D.J.: The Pulse of Calm Fan Deltas. The Journal of Geology, 11(4), 315-330; http://dx.doi.org/10.1086/588830, 2008.

Lane, E. W.: Importance of fluvial morphology in hydraulic engineering, Proceedings of the American Society of Civil Engineers, 81, 1–17, 1955.

Larson P.H., Dorn R.I., Faulkner D.J., and Friend d.A.: Toe-cut terraces: A review and proposed criteria to differentiate from traditional fluvial terraces. Progress in Physical Geography, v. 39(4), 417–439, 2015.

Leeder M.R., and Mack G.H.: Lateral erosion ("toe-cutting") of alluvial fans by axial rivers: implications for basin analysis and architecture. Journal of the Geological Society, London, v. 158, 885-893, 2001.

Leopold, L.B., and Maddock, T. Jr.: The Hydraulic Geometry of Stream Channels and Some Physiographic Implications. Geological survey professional paper 252, 1953.

Lupker, M., Blard, P., Lavé, J., France-Lanord, C., Leanni, L.,Puchol, N., Charreau, J., and Bourlès, D.: ^{10}Be-derived Himalayan denudation rates and sediment budgets in the Ganga basin. Earth and Planetary Science Letters, 333–334, 146–156, doi: http://dx.doi.org/10.1016/j.epsl.2012.04.020, 2012.

Mackin J.H.: Concept of the graded river. Bulletin of the Geological Society of America, v. 69, 463-512, 1948.

Mather A.E., Stokes M., and Whitfield E.: River terraces and alluvial fans: The case for an integrated Quaternary fluvial archive. Quaternary Science Reviews, v. 166, 74-90; http://dx.doi.org/10.1016/j.quascirev.2016.09.022; 2017.

Meyer-Peter, E. and Müller, R.: Formulas for Bed-Load Transport, in: 2nd Meeting of the International Association for Hydraulic Structures Research, 7–9 June 1948, Stockholm, Sweden, International
Association for Hydraulic Structures Research, 39–64, 1948.

Miller, J.P.: High Mountain Streams: Effects of Geology on Channel Characteristics and Bed Material. State bureau of mines and mineral resources New Mexico institute of mining and technology Socorro, New Mexico. Memoir 4, 1958.

Mouchené, M., van der Beek, P., Carretier, S., and Mouthereau, F.: Autogenic versus allogenic controls on the evolution of a coupled fluvial megafan–mountainous catchment system:

numerical modelling and comparison with the Lannemezan megafan system (northern Pyrenees, France). Earth Surf. Dynam., 5, 125–143, doi:10.5194/esurf-5-125-2017, 2017.

Nicholas, A.P., Quine, T.A.: Modeling alluvial landform change in the absence of external environmental forcing. Geology, v. 35(6), 527–530; doi: 10.1130/G23377A.1, 2007.

Nicholas, A. P., Clarke L., and Quine T. A.: A numerical modelling and experimental study of flow width dynamics on alluvial fans. Earth Surf. Process. Landforms 34, 1985–1993; DOI: 10.1002/esp.1839;, 2009.

Paola, C., Straub, K., Mohrig, D., and Reinhardt L.: The "unreasonable effectiveness" of stratigraphic and geomorphic experiments. Earth-Science Reviews, v. 97(1–4), 1-43, https://doi.org/10.1016/j.earscirev.2009.05.003, 2009.

Parker, G.: Hydraulic geometry of active gravel rivers, J. Hydraul. Div., 105, 1185–1201, 1978.

Parker, G.: Progress in the modeling of alluvial fans, Journal of Hydraulic Research, 37(6), 805-825, http://dx.doi.org/10.1080/00221689909498513, 1999.

Parker, G. Paola, C., Whipple, K.X., and Mohrig, D.: Alluvial fans formed by channelized fluvial
And sheet flow. I: Theory. Journal of Hydraulic Engineering, v. 124(10), 1998.

Pepin, E., Carretier, S., and Herail, G.: Erosion dynamics modelling in a coupled catchment–fan system with constant external forcing. Geomorphology, v. 122, 78–90, doi:10.1016/j.geomorph.2010.04.029, 2010.

Reitz, M.D., Jerolmack, D.J., and Swenson J.B.: Flooding and flow path selection on alluvial fans and deltas. Geophysical Research Letters, v. 37, L06401, doi:10.1029/2009GL041985, 2010.

Reitz, M.D., and Jerolmack, D.J.: Experimental alluvial fan evolution: Channel dynamics, slope controls, and shoreline growth. Geophysical Research Letters, v. 117, F02021, doi:10.1029/2011JF002261, 2012.

Rice, S.P., and Church, M.: Longitudinal profiles in simple alluvial systems. Water Resources Research, v. 37(2), 417-426, 2001.

Rice, S.P., Kiffney, P., Greene, C., and Pess, G.R.: The ecological importance of tributaries and confluences. In: River Confluences, Tributaries and the Fluvial Network © John Wiley & Sons, Ltd. ISBN: 978-0-470-02672-4, 2008.

Ritter, J.B., Miller, J.R., Enzel, Y., and Wells, S.G.: Reconciling the roles of tectonism and climate in Quaternary alluvial fan evolution. Geology, v. 23(3), 245–248, 1995.

Rohais, S., Bonnet, S., and Eschard, R.: Sedimentary record of tectonic and climatic erosional perturbations in an experimental coupled catchment-fan system. Basin Research, v. 24, 198–212, doi: 10.1111/j.1365-2117.2011.00520.x, 2012.

Savi, S., Norton, K. P., Picotti, V., Akçar, N., Delunel, R., Brardinoni, F., Kubik, P., and Schlunegger, F.: Quantifying sediment supply at the end of the last glaciation: Dynamic reconstruction of an alpine debris-flow fan, GSA Bull., 126, 773–790, https://doi.org/10.1130/B30849.1, 2014.

Savi, S., Schildgen T. F., Tofelde S., Wittmann H., Scherler D., Mey J., Alonso R. N., and Strecker M. R.: Climatic controls on debris-flow activity and sediment aggradation: The Del Medio fan, NW Argentina, J. Geophys. Res. Earth Surf., 121, 2424–2445, doi:10.1002/2016JF003912, 2016.

Schildgen, T. F., Robinson, R. A. J., Savi, S., Phillips, W. M., Spencer, J. Q. G., Bookhagen, B., Scherler, D., Tofelde, S., Alonso, R. N., Kubik, P. W., Binnie, S. A., and Strecker, M. R.: Landscape response to late Pleistocene climate change in NW Argentina: Sediment flux modulated by basin geometry and connectivity, J. Geophys. Res.-Earth, 121, 392–414, https://doi.org/10.1002/2015JF003607, 2016.

Schumm, S. A.: Geomorphic thresholds and complex response of drainage systems, Fluv. Geomorphol., 6, 69–85, 1973.

Schumm, S. A. and Parker, R. S.: Implication of complex response of drainage systems for Quaternary alluvial stratigraphy, Nat. Phys. Sci., 243, 99–100, 1973.

Schwanghart, W. and Scherler, D.: Short Communication: TopoToolbox 2 – MATLAB-based software for topographic analysis and modeling in Earth surface sciences, Earth Surf. Dynam., 2, 1-7, https://doi.org/10.5194/esurf-2-1-2014, 2014.

Simon, A., and Rinaldi, M.: Channel instability in the loess area of the midwestern United States. Journal of the American Water Resources Association, v. 36(1), Paper No. 99012, 2000.

Straub, K.M., Paola, C., Mohrig, D., Wolinsky, M.A., and George, T.: Compensational stacking of channelized sedimentary deposits. Journal of Sedimentary Research, v. 79, 673–688, doi: 10.2110/jsr.2009.070, 2009.

Tofelde, S., Savi, S., Wickert, A. D., Bufe, A., and Schildgen, T. F.: Alluvial channel response to environmental perturbations: fill-terrace formation and sediment-signal disruption, Earth Surf. Dynam., 7, 609-631, https://doi.org/10.5194/esurf-7-609-2019, 2019.

Van den Berg van Saparoea, A.P. H., and Postma, G.: Control of climate change on the yield of river systems, Recent Adv. Model. Siliciclastic Shallow-Marine Stratigr. SEPM Spec. Publ., 90, 15–
33, 2008.

Van Dijk, M., Postma, G., and Kleinhans, M.G.: Autocyclic behaviour of fan deltas: an analogue experimental study. Sedimentology, v. 56, 1569–1589, doi: 10.1111/j.1365-3091.2008.01047.x, 2009.

Van Dijk, M., Kleinhans, M.G., Postma, G., and Kraal, E.: Contrasting morphodynamics in alluvial fans and fan deltas: effect of the downstream boundary. Sedimentology, v. 59, 2125–2145 doi: 10.1111/j.1365-3091.2012.01337.x, 2012.

Von Blanckenburg, F.: The control mechanisms of erosion and weathering at basin scale from cosmogenic nuclides in river sediment. Earth and Planetary Science Letters, v. 237, 462–479, 2005.

Whipple, K.X., Parker, G. Paola, C., and Mohrig, D.: Channel Dynamics, Sediment Transport, and the Slope of Alluvial Fans: Experimental Study. The Journal of Geology, v. 106, 677–693, 1998.

Whipple, K.X., and Tucker, G.E.: Implications of sediment-flux-dependent river incision modelsfor landscape evolution. Journal of Geophysical Research, 107, B2, 2039, doi: 10.1029/2000JB000044, 2002.

Wickert, A. D. and Schildgen, T. F.: Long-profile evolution of transport-limited gravel-bed rivers, Earth Surf. Dynam., 7, 17–43, https://doi.org/10.5194/esurf-7-17-2019, 2019.

Wittmann, H., and von Blanckenburg, F.: Cosmogenic nuclide budgeting offloodplain sediment transfer. Geomorphology, 109, 246-256, 2009.

Wittmann, H., von Blanckenburg, F., Maurice, L., Guyot, J., Filizola, N., and Kubik, P.W.: Sediment production and delivery in the Amazon River basin quantified by in situ–produced cosmogenic nuclides and recent river loads. GSA Bulletin, 123 (5-6), 934–950, doi: https://doi.org/10.1130/B30317.1, 2011.